INSTITUTO POTOSINO DE INVESTIGACIÓN CIENTÍFICA Y TECNOLÓGICA, A.C.

POSGRADO EN CIENCIAS EN BIOLOGIA MOLECULAR

Chromatin remodeling protein Abf1 regulates expression of adhesin encoding genes in *Candida glabrata*

Tesis que presenta

Grecia Hernández Hernández

Para obtener el grado de

Doctora en Ciencias en Biología Molecular

Directora de la Tesis:

Dra. Irene B. Castaño Navarro

San Luis Potosí, S.L.P., Julio 2024

Constancia de aprobación de la tesis

La tesis "**Chromatin remodeling protein Abf1 regulates the expression of adhesin encoding genes in *Candida glabrata***" presentada para obtener el Grado de Doctor(a) en Ciencias en Biología Molecular fue elaborada por **Grecia Hernández Hernández** y aprobada el **05 de Julio de 2024** por los suscritos, designados por el Colegio de Profesores de la División de Biología Molecular del Instituto Potosino de Investigación Científica y Tecnológica, A.C.

_____

Dra. Irene B. Castaño Navarro
Directora de la tesis

_____

Dra. Lina R. Riego Ruíz
Miembro del Comité Tutoral

_____

Dr. Gerardo Argüello Astorga
Miembro del Comité Tutoral

_____

Dr. Roberto Sánchez Olea
Miembro del Comité Tutoral

Créditos Institucionales

Esta tesis fue elaborada en el Laboratorio de Microbiología Molecular de la División de Biología Molecular del Instituto Potosino de Investigación Científica y Tecnológica, A.C., bajo la dirección de la Dra. Irene B. Castaño Navarro, apoyada por los proyectos CB-2014 No. 239629 y CF-2019 No. 610281

Durante la realización del trabajo el autor recibió una beca académica del Consejo Nacional de Humanidades, Ciencias y Tecnologías (712172) y del Instituto Potosino de Investigación Científica y Tecnológica, A. C.

Página en Blanco que se va a utilizar para colocar la copia del acta de examen.

Dedicatorias

A mis abuelos **Ramona** e **Inés**, por enseñarme el verdadero significado de la vida y porque sin ellos no estaría aquí hoy.

A mi madre **Rosario**, por todo su amor y sacrificios que hicieron posible para que yo pudiera seguir mis sueños, sin ella esto no sería posible.

A mi padre **Horacio**, por siempre estar para apoyarme, por enseñarme e impulsarme en todo.

A **Cielo**, simplemente por estar y existir, por ser la mejor cómplice de la vida.

A **Fermín**, por apoyarme, por creer en mí y ver en mí más de lo que yo imagine, por ser mi compañero de aventuras.

A **Luz** y **Fermín**, por adoptarme también como su familia y apoyarme, este logro también es suyo.

Finalmente, a mis compañeros de cuatro patas: **Mika, Pelusa, Trip, Ciruela, Max, Quilla, Taz y Gordita,** por siempre sacarme una sonrisa y ser la definición de amor incondicional.

♥

Agradecimientos

Al CONHACYT por la beca otorgada, al Instituto Potosino de Investigación Científica y Tecnológica, A.C., y al Laboratorio Nacional de Biotecnología Agrícola, Médica y Ambiental (LANBAMA), por los servicios brindados.

A la Dra. Irene Castaño Navarro, por todas sus enseñanzas. Por ser un ejemplo de cómo persona y científica. Por confiar en mí, por sembrar y nutrir en mí el bello mundo de la ciencia. Gracias infinitas. ♥

Al Dr. Alejandro De Las Peñas Nava por sus enriquecedores comentarios que contribuyeron a mi formación académica.

Al Dr. Gerardo Argüello Astorga, al Dr. Roberto Sánchez Olea y la Dra. Lina Riego Ruiz por sus valiosos comentarios y sugerencias que enriquecieron este trabajo.

A la Dra. Ma. Guadalupe Gutiérrez Escobedo por enseñarme cada una de las técnicas del laboratorio, y excelentes consejos.

A la Dra. Karina Robledo Márquez por su apoyo y consejo técnico, por su tiempo y amistad.

Al Dr. Nicolas Gómez Hernández por su apoyo y asesoría técnica.

Al Dr. Saúl Jijón por su asesoría técnica.

A Gloria López Niño por todo su apoyo que hizo posible cada uno de los experimentos.

A M.C. Daniel Rafael Saldaña por su apoyo técnico con Rstudio.

A todos mis compañeros que han formado parte y a los que continúan en el laboratorio 6 de Microbiología Molecular, en especial a Lupita, Mariana, Belén, Lau, Lily, Yaz y Alex por compartir sus conocimientos, tiempo y amistad conmigo. ♥

TABLE OF CONTENTS

List of tables

List of figures

Resumen

El arreglo espacial del ADN dentro del núcleo juega un papel fundamental en la regulación de la expresión de genes, y está en función de los estímulos externos a los que está sujeto el organismo. En el caso de hongo patógeno oportunista *Candida glabrata* (*Nakaseomyces glabrata*) la estructura tridimensional juega un papel fundamental en su éxito para colonizar nichos dentro de su hospedero. La adhesión a células epiteliales, una característica importante para su virulencia depende principalmente del gen *EPA1* que codifica para la proteína de pared Epa1 y cuya expresión está sujeta a silenciamiento subtelomérico. En *C. glabrata* el silenciamiento subtelomérico depende principalmente de las proteínas del complejo SIR, yKu70/yKu80, *Cg*Rap1 y *Cg*Abf1. Previamente en el laboratorio encontramos que el telómero E derecho donde se encuentran los genes *EPA1*, *EPA2* y *EPA3*, puede formar estructuras secundarias tipo asa a través de elementos en *cis* como el protosilenciador Sil2126, el Elemento Negativo (NE) y otras regiones intergénicas. En este trabajo encontramos mediante ensayos de inmunoprecipitación de la cromatina (ChIP-qPCR), que *Cg*Rap1 y *Cg*Abf1 se unen en diferentes posiciones a lo largo de este telómero. Principalmente encontramos que *Cg*Abf1 se une a la región que comprende el promotor de *EPA1* en dos sitios diferentes, lo cual sugiere que *Cg*Abf1 regula la expresión de *EPA1*. También, definimos las secuencias que constituyen los motivos de unión para las proteínas *Cg*Abf1 y *Cg*Rap1 en *C. glabrata* utilizando herramientas bioinformáticas, y evaluamos la expresión de *EPA1* por RT-qPCR en el fondo mutante *Cgabf1-43* (que carece de los últimos 43 aminoácidos en su carboxilo terminal). Observamos un aumento del transcrito de *EPA1* en esta cepa y un incremento en la adhesión a células HeLa. Además, encontramos que la proteína *Cg*Abf1 puede interaccionar con otras proteínas del silenciamiento como Sir3, Sir4, *Cg*Rap1 y yKu70/80, mediante ensayos de co-inmunoprecipitación.

Por otro lado, encontramos focos de Sir4 y yKu70 distribuidos en la periferia nuclear lo cual sugiere un anclaje de los telómeros en esta región que podría contribuir al silenciamiento.

Palabras clave: adhesinas, *EPA1*, *Cg*Abf1, *Cg*Rap1, cromatina, telómero, silenciamiento.

Abstract

The DNA spatial arrangement inside the nucleus critically depends on external stimuli and plays a fundamental role in gene expression. In the fungal opportunistic pathogen *Candida glabrata* (*Nakaseomyces glabrata*), gene regulation plays an essential role on its ability to colonize and disseminate within the host, partly through the regulation of the expression of adhesins' that are involved in its adherence to epithelial cells. This characteristic largely depends on the gene *EPA1* gene, which is subject to subtelomeric silencing and encodes the cell wall protein Epa1. Subtelomeric silencing in *C. glabrata* depends on the SIR complex, yKu70/yKu80, *Cg*Rap1, and *Cg*Abf1. Moreover, we previously found that the E-R telomere, that harbors the genes *EPA1*, *EPA2*, and *EPA3*, can be remodeled into loop-like secondary structures through the interaction of *cis*-acting elements like the protosilencer Sil2126, the Negative Element (NE), and other intergenic regions. In this work, we found that Rap1 and Abf1 proteins bind at different positions throughout this telomere using chromatin immunoprecipitation assays (ChIP-qPCR). Moreover, we found that *Cg*Abf1 binds near the promoter region of *EPA1* at two different positions, and that *EPA1* expression is negatively regulated by Abf1. Consistently, the truncated mutant *Cgabf1-43* (that lacks the last 43 amino acids at its C-terminal) displayed an increase in *EPA1* transcript and cells were more adherent to epithelial cells *in vitro* compared to the parental strain. We also determined the binding sequences for Abf1 and Rap1 in *C. glabrata*, using the data from the ChIP assays and bioinformatic tools. Additionally, we found that *Cg*Abf1 co-immunoprecipitates with other silencing proteins like *Cg*Rap1, Sir3, Sir4, yKu70/80, which suggests their interaction.

Furthermore, we observed that Sir4 and yKu70/80 colocalized with the nuclear periphery which suggests that the telomeres might be localized at this region thereby reinforcing the silencing of the genes adjacent to the telomere.

Key words: Adhesins, *EPA1*, *Cg*Abf1, *Cg*Rap1, chromatin, telomere, silencing.

1. Introduction

1.1. Chromatin organization

Inside the nuclei the DNA is not disposed randomly; instead, chromosomes are compartmentalized into specific regions within the nucleus which allows individual regions of the chromosomes to interact with other distant regions within the same chromosome or in other chromosomes. Different chromatin compartments can be visualized within the nuclei at different stages during the cell cycle, these compartments are called chromosome territories. Inside these chromosome territories, spatial organization of chromatin is dynamic, and crucial for gene regulation, recombination, repair, and other processes that involve DNA maintenance (Sexton et al., 2012). The structural conformations of intra-chromosome and inter-chromosome interactions are known as topologically associated domains (TADs) that lead to three-dimensional organization within a specific chromosome territory. This organization creates distinct chromatin states, that also exhibit a dynamic response to multiple cellular processes, the boundary elements or *cis*-acting elements that function as barriers and limit distinct chromatin domains helps to shape the expression pattern within a chromosome territory (Fig. 1). For instance, a fraction of DNA is folded into heterochromatin, which is a condensed state of chromatin that is transcriptionally inactive, and euchromatin is more accessible to the transcription machinery (Beisel and Paro, 2011). Moreover, the specialized structures at the end of chromosomes, the telomeres, are normally arranged into clusters localized within the nuclear periphery (Cockell et al., 1995; Palladino et al., 1993). The specialized structures adjacent to telomeres, called the subtelomeres, are also near the nuclear periphery which also affects transcription of the genes encoded within these regions (Lebrun et al., 2001).

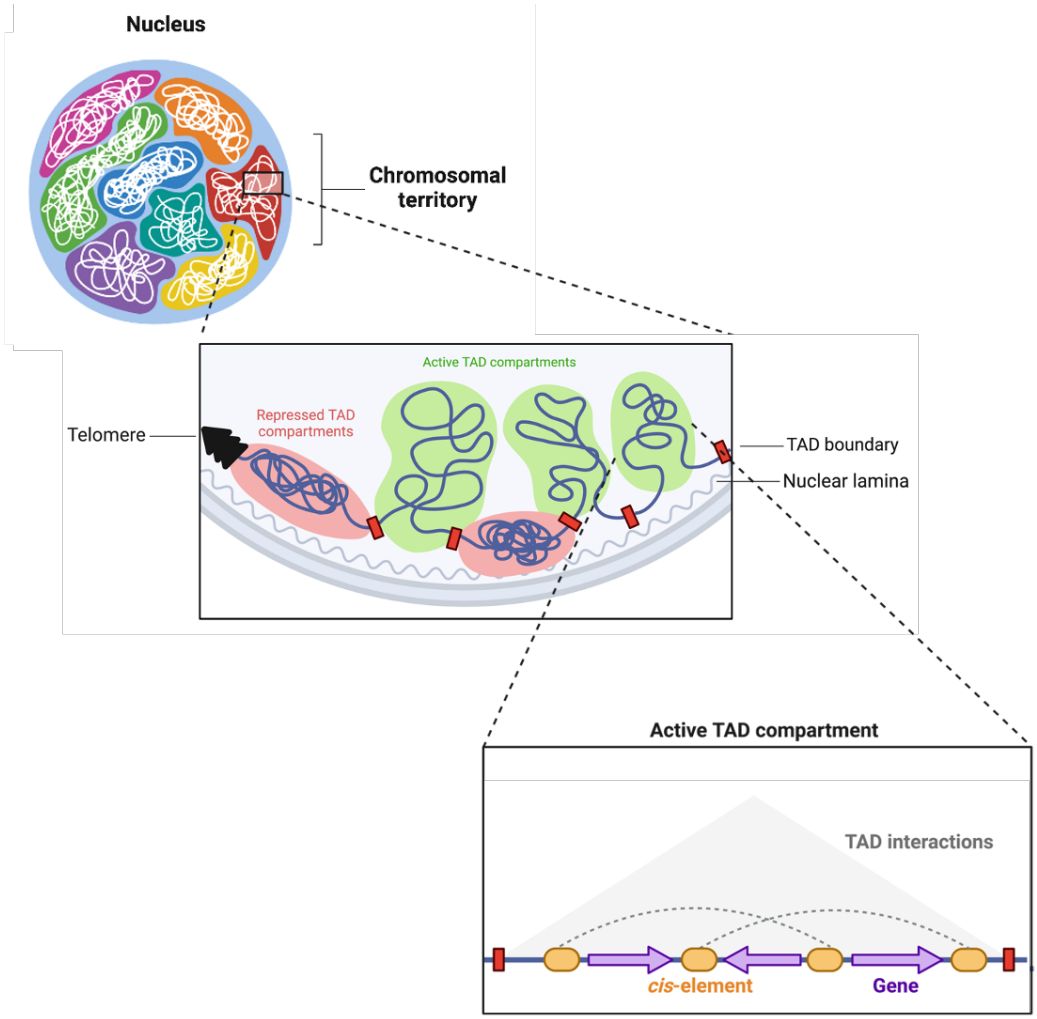

Figure 1 Chromosomal architecture and functional domains in the DNA. Chromatin inside the nucleus is organized into different subcomparments known as chromosome territories. Within these territories topologically associated domains (TADs) can be found. TADs can group depending on the role they perform in the cell; for example, within a same chromosomal territory active or repressed TADs can be found. Interactions between different TADs play an important role in regulating gene expression and other DNA metabolic processes, these interactions depend on *cis*-acting elements that can regulate genes located far away.

1.2. Telomeres are specialized structures at the end of the chromosomes

Telomeres consist of non-coding tandem repeated sequences and a G-rich strand that extends to form a 3' single tail or G tail. With every cell cycle, G tails are shortened. Telomeres are deprived of nucleosomes, instead a complex of several proteins binds to these sequences and protect the integrity of the ends of the

chromosomes from degradation, fusion, and recombination events (Pfeiffer and Lingner, 2013; Teixeira and Gilson, 2005; Zaman et al., 2002).

In the baker's yeast *Saccharomyces cerevisiae,* there are several proteins associated with the telomeres, most of which are involved in multiple cellular processes. Telomeric repeats contain high affinity binding sites for Rap1 (Repressor activator protein 1). Association of Rap1 to telomeres is key to prevent telomere fusions and maintenance of telomere length (Conrad et al., 1990). Rap1 recruits SIR proteins (Silence Information Regulator) Sir3, and Sir4 at the telomeres and promote transcriptional silencing known as TPE (Telomere Position Effect). Sir2, also part of the SIR complex, is a NAD-dependent histone deacetylase essential for repression which contributes to propagate silencing from the telomeric repeats to the subtelomeric region (Gottschling et al., 1990; Luo et al., 2002; Moretti and Shore, 2001). Rap1 also interacts with proteins Rif1/2 (Rap1 interaction factor 1 and 2), and together maintain telomere length, and participate in heterochromatin spreading. Furthermore, Rap1-Rif2 interaction prevents telomere fusions (Bonetti et al., 2010; Hardy et al., 1992; Wotton and Shore, 1997). Another important complex yKU formed by yKu70 and yKu80 (yKu70/80) binds at the end of telomeres and is essential for DNA repair via non-homologous end joining (NHEJ) and requires the SIR complex. Moreover, yKU complex is involved in the stability of the telomere length, protection of the telomeres from recombination, promotion of TPE and telomere tethering to the nuclear envelope (Boulton and Jackson, 1998, 1996; Cosgrove et al., 2002; Gravel and Wellinger, 2002). During the cell cycle foci of associated telomere-proteins like Rap1, Sir4 and yKu complex, can be observed near the nuclear periphery. Peripheral localization varies from telomere to telomere and it does not always require Sir3, yKu70 or Rap1; instead, there is another pathway that leads the localization of telomeres near the nuclear periphery that depends on Esc1 (Establishes Silent Chromatin), which is located at the inner face of the nuclear envelope and interacts with the Sir4-PAD domain (Andrulis et al., 2002; Taddei et al., 2004). Tethering of telomeres via this pathway to the nuclear periphery not only requires Esc1-Sir4 interaction but also yKu80, this association of telomeres to the nuclear periphery through Esc1-Sir4 interaction promotes and maintains silent chromatin (Taddei et al., 2004).

1.3. Establishment of subtelomeric silencing

Subtelomeric regions harbor very few coding genes and exhibit high variability that makes them hotspots for recombination events, both within and between chromosomes, which can lead to genomic rearrangements, gene duplications, and genetic diversity. Plasticity at the subtelomeric region allows organisms to adapt to different environmental conditions, shaping genome architecture and driving species divergence (Ai et al., 2002; Fabre et al., 2005; Fourel et al., 1999).

Transcriptional silencing at the regions adjacent to telomeres, known as TPE, is a form of regional repression that starts with Rap1 binding at telomeres, and its interaction with Sir4 through the Rap1 C-terminal region, initiating the assembly of Sir2-Sir3 at the nucleosomes that continuously spreads repressed chromatin from the telomere (Fig. 2). Sir2 deacetylase activity at histones H3 and H4 creates high affinity binding sites for Sir3 and Sir4 which helps propagate silent chromatin, specifically deacetylation of H4K16 allows Sir3 and Sir4 binding the H3 and H4 N-terminal tails. Previous work had shown that SIR complexes bound throughout the telomere are able to fold and shape chromatin into higher-order structures. Also, the yKU complex plays a crucial role in Sir4 the recruitment and silenced chromatin establishment (Kirkland et al., 2015; Luo et al., 2002; Strahl-Bolsinger et al., 1997). In *S. cerevisiae*, heterochromatin assembly is also found at *HML* and *HMR* mating loci that are flanked by E and I silencers that harbor binding sites for Rap1, Abf1 (ARS-binding factor 1) and ORC complex (Origin of Recognition Complex). Abf1 interacts with Sir3 while ORC interacts with Sir1 leading to the assembly of Sir2, and Sir4 which are crucial for establishment of full repression of the *HM* loci (Rine et al., 1979; Rine and Herskowitz, 1987). While Sir2, 3 and 4 are frequently associated with sequences at the *HMR-E* and *HMR-I* silencers, Sir1 is associated only with the *HMR-E* silencer, successive rounds of SIR complex binding shape the chromatin into a loop that leads to a compact structure (Rusché et al., 2002).

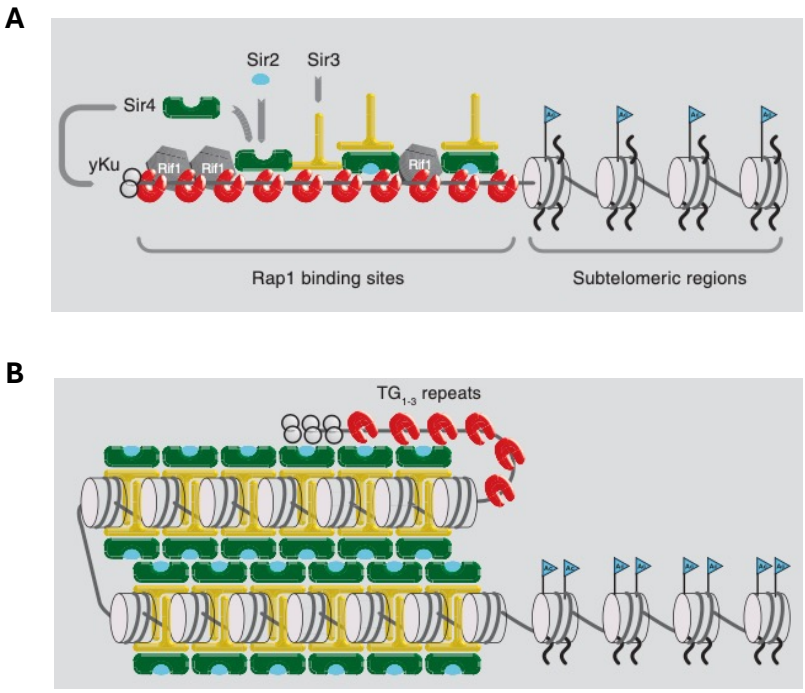

Figure 2 Model for heterochromatin assembly in *S. cerevisiae*. A; Schematic representation of silencing complex assembly, where Sir4 binds to Sir2-3 to repeated sequences at the telomere where also Rap1 and yKu bind. B; Silencing complexes spread to the adjacent region closest to the telomere folding into higher-order heterochromatin. Modified from (Grunstein and Gasser, 2013)

Additionally, it has been shown that silent *HML* and *HMR* loci are closely associated with telomeres at nuclear envelope. Silent chromatin anchoring to nuclear periphery is driven by Sir4 interaction with the nuclear envelope associated protein Esc1 This interaction allows localization of Sir-repressed chromatin domain at perinuclear sites (Fig. 3) (Andrulis et al., 2002, 1998). Besides, there is another pathway to tether telomeres to nuclear periphery that involves yKU complex even in the absence of silencing, but anchoring requires yKu-Sir4 interaction (Taddei et al., 2004).

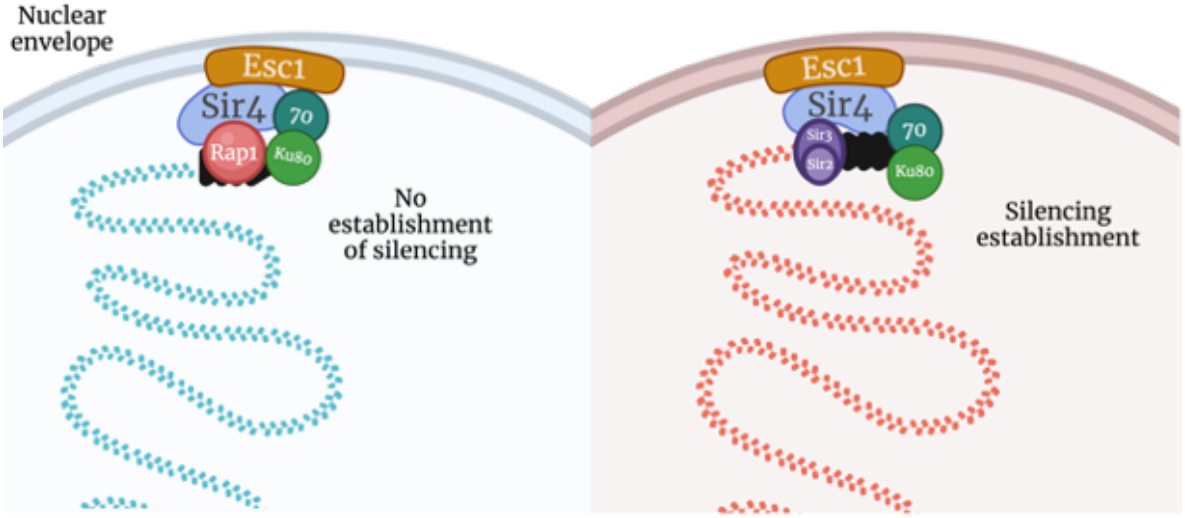

Figure 3 Pathways for telomere tethering at the nuclear envelope in *S. cerevisiae*. Left, representation of telomere tethering at the nuclear envelope that depends on Sir4 and Rap1 recruitment through the interaction with Esc1. In this pathway, silencing is not triggered by telomere anchoring to the NE. Right, representation of telomere tethering at the nuclear envelope that depends on Sir4 and yKu complex interaction with Esc1. This telomere anchoring contributes to the establishment of silencing and involves SIR protein complex (right). Modified from (Taddei et al., 2004).

1.4. *Cis*-acting elements

Temporal and spatial conformation of DNA is a critical aspect that regulates nuclear functions in eukaryotes. Chromatin hierarchical organization allows distant fragments of DNA to interact with each other through DNA loops. This interaction depends on non-coding sequences mostly known as *cis*-acting elements like enhancers, promoters, and silencers that contain binding sites for different *trans*-regulatory elements such as transcription factors (TFs) that lead to the interaction of distal elements with its target genes (Beisel and Paro, 2011; Grunstein and Gasser, 2013; Hediger and Gasser, 2002; Taddei et al., 2004). In addition, *cis*-regulatory sequences play a central role in evolution where changes in these elements have been shown to be important in phenotypic divergence. Gene expression patterns can be altered by TFs and their interaction with promoters, which also depend on nucleosome positioning or rearrangement relative to the binding of the TF (Wittkopp and Kalay, 2012).

S. cerevisiae telomeres of function as silencers which are a type of *cis*-regulatory element, that harbor high affinity sequences for Rap1 that are key in the nucleation of the silencing machinery (Buck and Shore, 1995; Marcand et al., 1997). Also, *HM*

loci are flanked by silencers that act as “barrier elements” that limit the silencing activity to the *HM* loci (Boscheron et al., 1996).

1.5. Chromatin remodeling proteins Abf1 and Rap1

Chromatin remodeling proteins are crucial components in the expression of genes, genome stability, and other DNA metabolic processes. Among these proteins, Abf1 and Rap1 are key factors in *S. cerevisiae* which significantly influence the chromatin organization and function and are necessary to trigger specific metabolic functions such as regulation of carbon source utilization, sporulation, and ribosomal function. *Sc*Abf1 and *Sc*Rap1 have conserved amino acid residues at their trans-activation and silencing domains, which suggests that these regions may share similar mechanisms to mediate silencing and transcriptional activation (Miyake et al., 2002; Yarragudi et al., 2004).

1.5.1. Abf1

Autonomously replicating sequence (ARS)-binding factor 1 (Abf1) is an abundant zinc finger transcription factor that plays pivotal roles in numerous cellular processes and is essential for cell viability. Abf1 is a general transcription factor (GTF) that is involved in the regulation of at least 86 genes in *S. cerevisiae*, which represents 1.4% of the total genome, 50 of them are activated and 36 are transcriptionally repressed by Abf1. Genes regulated by Abf1 participate in many cellular pathways like ribosome biogenesis, and cellular respiration (Fermi et al., 2016; Planta, 1997; Rhode et al., 1989a; Rie Gailus-Durner et al., 1996). For instance, *COX6* which encodes a subunit of cytochrome c oxidase (essential in mitochondrial respiratory chain) has essential *cis*-elements that directly bind Abf1 regulating positively and negatively its transcription. Interestingly, it has been shown that this regulation depends on phosphorylation changes in Abf1 in response to glucose, where it is known that changes in the phosphorylation patterns of Abf1 affect the formation and abundance of protein-DNA complexes, therefore affecting the transcription of *COX6* (Trawick et al., 1992). Additionally, Abf1 transcription is affected by Cdc6 during S phase, where ORC can recruit Cdc6 at specific replicative origins, which establish and maintain the pre-replicative complex required at early steps in DNA replication

(Feng et al., 1998). Also, Abf1 can bind to its own promoter region and negatively regulate its own transcription (Fermi et al., 2016; Miyake et al., 2004).

Abf1 is key in chromatin remodeling and organization, it contributes to the formation of chromatin loops by binding to *cis*-acting elements thereby influencing the accessibility of transcription factors and other regulatory proteins. Abf1's C-terminal region is essential to mediate positive and negative transcriptional regulation, DNA replication, and silencing. In *S. cerevisiae* the C-terminal domain of Abf1 contains two crucial domains CS1 and CS2 (C-terminal sequence 1 and 2). CS1 consists of four essential amino acids which are required for the nuclear localization, mutants in CS1 are mislocated at the cytoplasm. CS2 domain consists of 23 amino acids that are required for inducing chromatin remodeling, influencing transcriptional activation, repression, and DNA replication (Miyake et al., 2002). *ScABF1* is required also for silencing of the *HML* and *HMR* mating type silent loci (Bi et al., 1999; Boscheron et al., 1996).

In *Candida glabrata*, which is relatively closely related phylogenetically to *S. cerevisiae*, *ABF1* is conserved and is also essential for cell viability. *Cg*Abf1 despite being a smaller protein (479 aa vs 731 aa of *Sc*Abf1), contains the main domains and these share a high percentage of identity with the corresponding *Sc*Abf1 domains. *Cg*Abf1 contains a bipartite DNA-binding domain composed of a Zinc finger domain (51 – 89 aa) at its N-terminal region and a DNA binding domain (201 – 371 aa). In addition, the C-terminal domain (438 – 453 aa) corresponds to the CS2 in *Sc*Abf1 which is highly conserved, and crucial to mediate subtelomeric silencing at different telomeres (Fig. 4A). Interestingly, the CS1 domain is not conserved in *Cg*Abf1. *Cg*Abf1 has multiple roles in DNA replication and cell cycle progression (Hernández-Hernández et al., 2021).

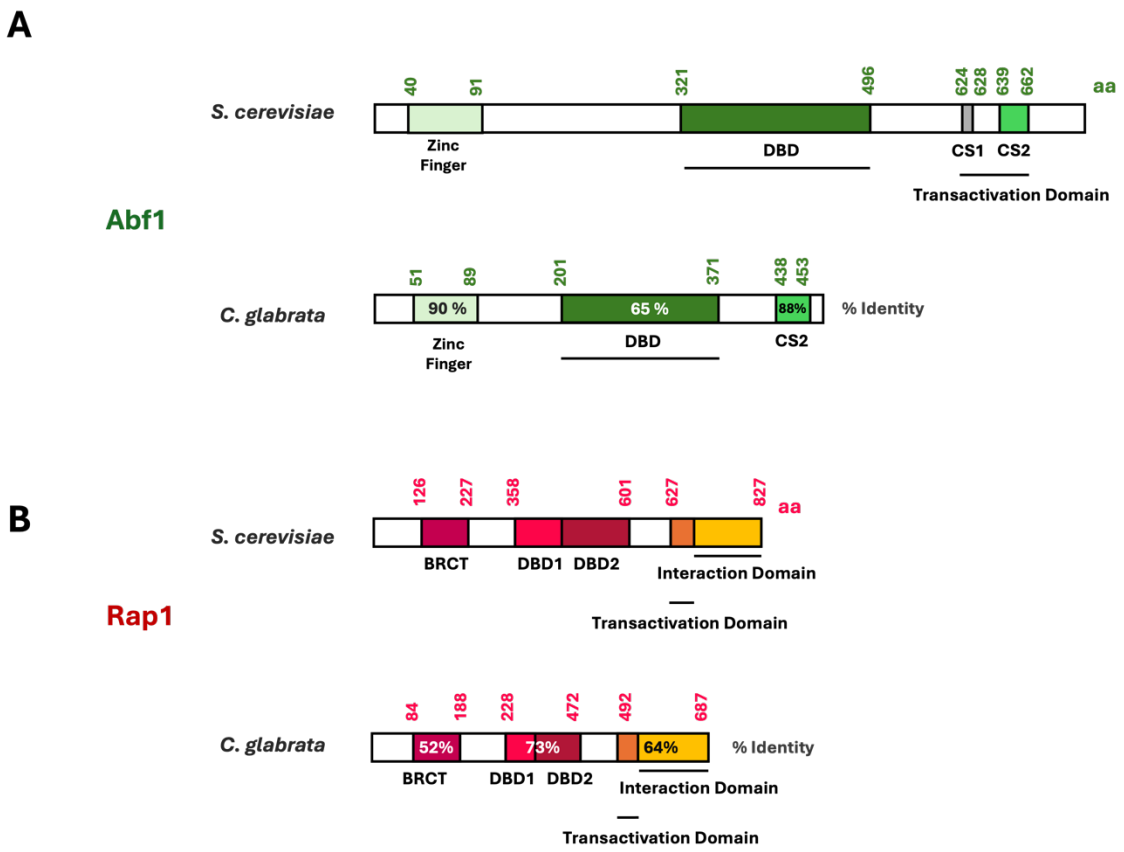

Figure 4 Chromatin remodeling proteins *Sc*Abf1 and *Sc*Rap1 are conserved in *C. glabrata*. A; Schematic representation of the *Sc*Abf1 domains and % identity of *Sc*Abf1 vs *Cg*Abf1. DBD: DNA binding domain, CS1-2: C-terminal sequence 1 and 2. B; Schematic representation of the *Sc*Rap1 domains and their % of identity in comparison with *Cg*Rap1. BRCT: BRCA1 C-terminus, DBD1-2: DNA binding domain (Hernández-Hernández et al., 2021; Kueng et al., 2013).

1.5.2. Rap1

Repressor-activator protein 1 (Rap1) is a multifunctional protein that was first discovered as a binding factor to both silencing and activation *cis*-elements in the budding yeast *S. cerevisiae*. Rap1 regulates genes involved in glycolysis, ribosomal protein genes, and deoxyribonucleotides synthesis genes (Elledge and Davis, 1989; Vignais et al., 1987). Rap1 is an abundant protein found at double stranded DNA at telomeric-repeats; nevertheless, about 90% of Rap1 is not telomere-associated (Gilson et al., 1993; Shore and Nasmyth, 1987). Rap1 has been shown to interact with Rif1/2 and together regulate telomere length. Telomere association with the nuclear periphery involves Rap1 foci formation, which contain yKu complex, Sir4 and Sir3 and are associated with 70% of the Y' telomere sequences (Hardy et al., 1992;

Levy and Blackburn, 2004; Palladino et al., 1993). In *S. cerevisiae,* Rap1 C-terminus is key for telomere maintenance and silencing and the interaction with Sir3/4 and Rif1/2 also depends on this domain (Buck and Shore, 1995).

In *C. glabrata,* Rap1 is relatively well conserved with *Sc*Rap1 (Fig. 4B) at the DNA binding and C-terminal domains. Deletion of the last 28 amino acids of *Cg*Rap1 C-terminal domain is unable to interact with Sir3 and therefore is defective for silencing. The *rap1-21* truncated allele results in the expression of many subtelomeric genes of which the majority belong to the *EPA* family of genes encoding the major adhesins in *C. glabrata* that are normally subject to subtelomeric silencing (De Las Peñas et al., 2003).

1.6. Silencing in *Candida glabrata*

C. glabrata (*Nakaseomyces glabrata*) is an opportunistic fungal pathogen that is commonly found as a commensal in the mucous membranes of healthy individuals. The World Health Organization (WHO) recently reported *C. glabrata* as a high priority risk fungal pathogen, due to its increased incidence in the last decades, as it is the second most isolated *Candida* spp after *Candida albicans*. Despite being associated with other *Candida* species, *C. glabrata* is phylogenetically more related to the budding yeast *S. cerevisiae* (Gabaldón et al., 2013).

Subtelomeric silencing in *C. glabrata* shares multiple similarities with the mechanism and machinery described in *S. cerevisiae.* For instance*,* SIR complex proteins Sir2, Sir3, and Sir4 are conserved in *C. glabrata* and required for subtelomeric silencing, as well Rap1, Abf1, and yKu proteins (De Las Peñas et al., 2003; Domergue et al., 2005; Hernández-Hernández et al., 2021; Ramírez-Zavaleta et al., 2010).

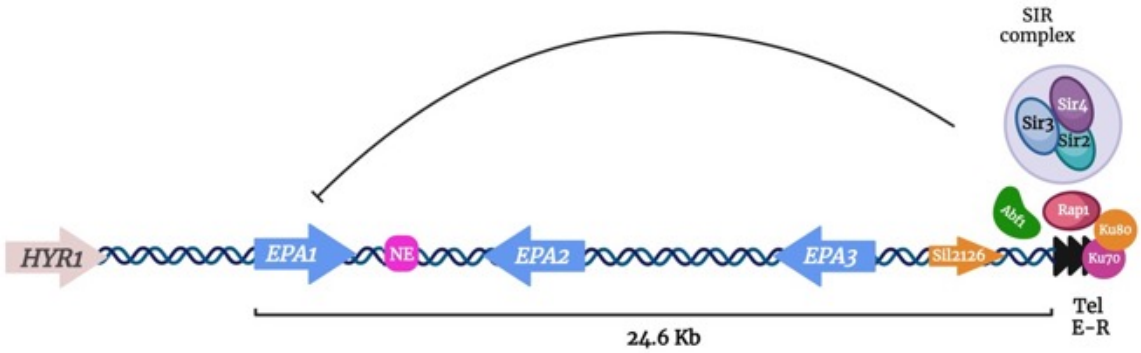

Figure 5 Subtelomeric silencing at telomere E-R where *EPA1, EPA2,* and *EPA3* form a cluster. Schematic representation of the telomere E-R where *EPA1, 2* and *3* are located, and are subject to subtelomeric silencing that depends on SIR complex, Rap1, Abf1, yKu70/80. Also shown are the *cis*-acting elements like the protosilencer Sil2126 and the negative element (NE), which are involved in the negative regulation of the adhesins at this telomere.

In *C. glabrata*, participation of the silencing machinery changes from telomere to telomere. At chromosome E-R where *EPA1, EPA2*, and *EPA3* form a cluster at the subtelomeric region, silencing depends mostly on SIR complex (Sir2,3, and 4), Rap1, Abf1, Rif1 (Rap1 interaction factor 1) and requires the *cis*-acting element Sil2126 found at the intergenic between *EPA3* and the telomere. Sil2126 requires Rap1 and Abf1 binding, and it has been proposed that Sil2126 interacts through protein-DNA interactions with other *cis*-elements found at the intergenic between *EPA2-EPA3* and *EPA1-EPA2*, which are important to remodel this telomere into different loop conformations that repress the expression of the genes located inside this structure (Hernández-Hernández et al., 2021; Juárez-Reyes et al., 2012;). In addition, *EPA1* is regulated by another *cis*-acting element called Negative Element (NE) located downstream *EPA1*, which represses its expression rapidly during log phase (Gallegos-García et al., 2012a) and requires yKu70/80. It is worth pointing out that yKU complex is not required for subtelomeric silencing at telomere E-R where *EPA1* is located (Rosas-Hernández et al., 2008).

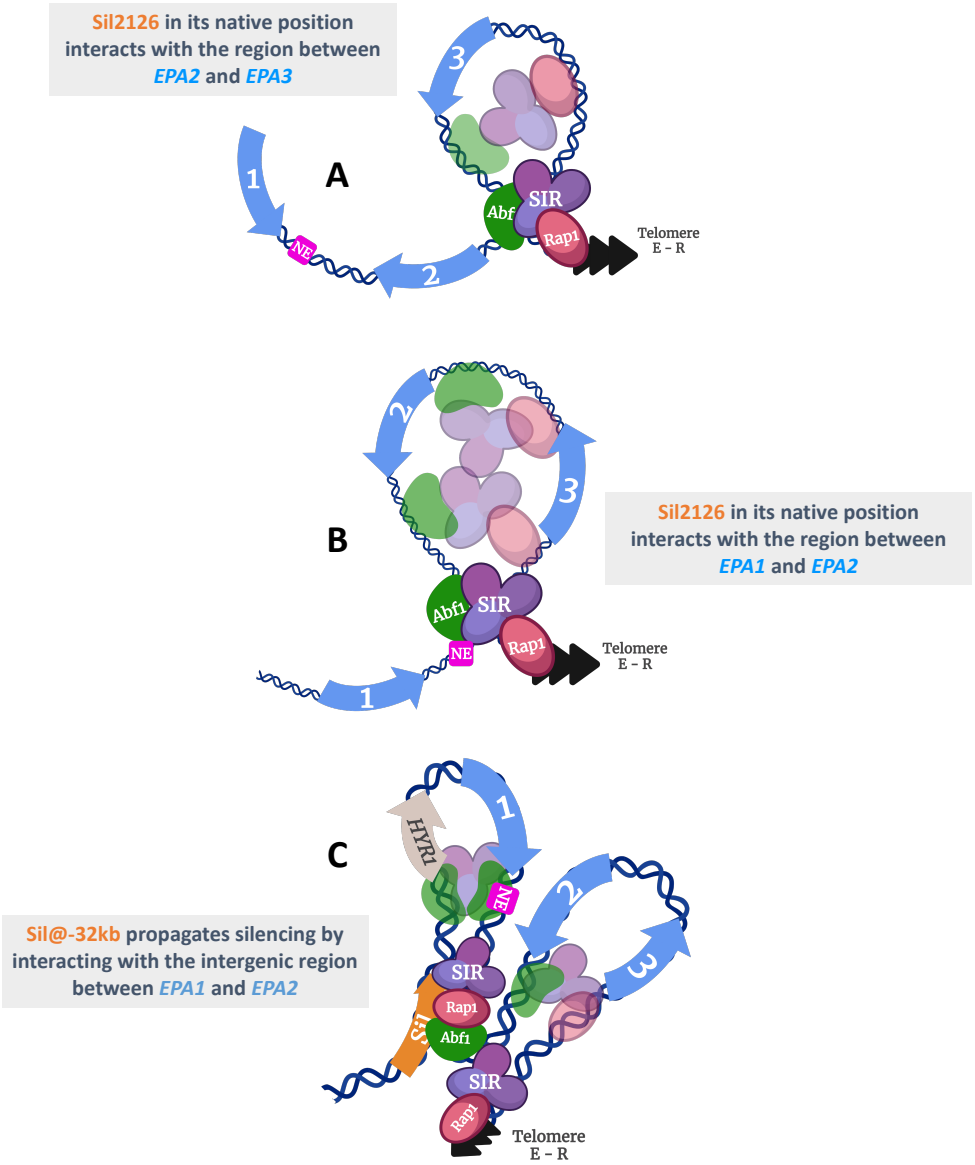

Figure 6 Chromatin loop formation that negatively regulates *EPA* genes in *C. glabrata*. A; Schematic representation of the interaction between the protosilencer Sil2126 at its original position (between *EPA3* and the telomere E-R) with the intergenic region of *EPA2-EPA3*. B; Schematic representation of the interaction of the protosilencer Sil2126 at its original position with the intergenic region of *EPA1-EPA2*. C; Schematic representation of the interaction of Sil2126 @-32 Kb from the telomere with *EPA1-EPA2* and *EPA3*-telomere intergenic regions.

Other adhesin-encoding genes like *EPA6* (Chr C-L, BG2 strain) and *EPA7* (Chr E-L, BG2 strain) are also subject to subtelomeric silencing which mostly depends on the SIR complex, Rap1, yKu70, and Rif1. Also, *EPA4* and *EPA5* located at telomere I-R are silenced and this silencing depends on the yKu complex (Rosas-Hernández et al., 2008).

1.7. Adhesins in *Candida glabrata:* a crucial virulence factor

C. glabrata's whole genome sequence of different strains has allowed to detect several structural changes in some chromosomes, like duplications and translocations, among others. These changes involve genes encoding glycosylphosphatidylinositol (GPI)-anchored adhesin-like proteins that confer adherence to a broad type of surfaces biotic or abiotic, which is a crucial virulence trait that makes it a successful pathogen.

Interestingly, most of this adhesin-like encoding genes are located at subtelomeric regions and contain highly repeated sequences that make them prone to rearrangements which could explain the expansion of adhesin-encoding genes in the *C. glabrata* genome. In BG2 standard laboratory strain, there are 81 genes encoding for cell surface proteins, and 26 adhesin-encoding genes that belong to the *EPA* (Epithelial Adhesins) family, which is the largest family of GPI-CWPs proteins (Fig. 7) (De Groot et al., 2008; Xu et al., 2020). In BG2 strain, Epa1 is the major adhesin responsible for 95% adherence to HEp2 epithelial cells *in vitro*, it requires Ca2+ and recognizes host glycoconjugates containing N-acetyl glucosamine (Cormack et al., 1999a).

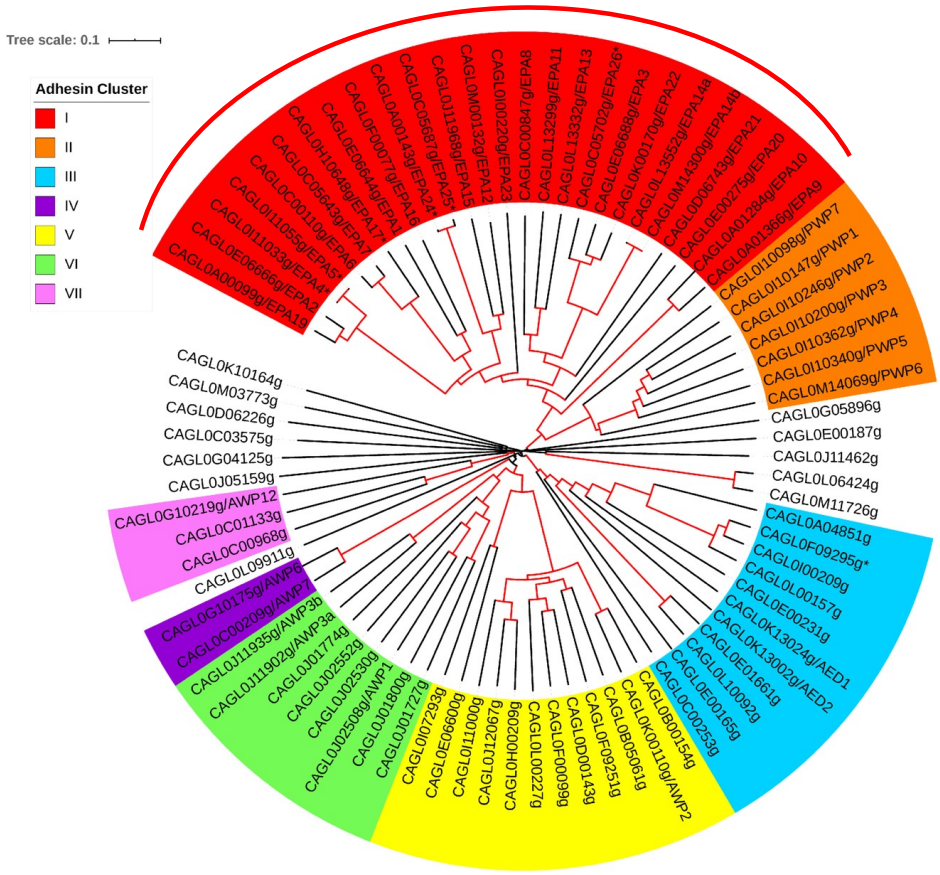

Figure 7 Cell wall protein-coding genes in *C. glabrata* (BG2). Phylogeny of the adhesin encoding genes which cluster into seven groups from the de novo assembly genome of BG2 genome, where the major adhesin cluster is the *EPA* family. Modified from (Xu et al., 2021).

In response to the environmental conditions, *C. glabrata* expresses different adhesins probably contributing to its survival and colonization within the host (Kraneveld et al., 2011a). For instance, Epa1, Epa6 and Epa7 are important to colonize the kidneys and bladder in a murine model; besides, Epa6 is important for biofilm formation on plastic surfaces (Castaño et al., 2005; De Las Peñas et al., 2003; Domergue et al., 2005). *EPA2*, found at telomere E-R, is induced in the presence of oxidative stress and is induced in the liver during host colonization, induction depends on Yap1 and Skn7 TFs (Juárez-Cepeda et al., 2015). *EPA3*, also found at Tel E-R, is important for biofilm formation and is induced under osmotic stress and glucose starvation (Kraneveld et al., 2011; Roetzer et al., 2008). Other adhesins like *EPA7* and *EPA22* are also expressed during biofilm formation (Kraneveld et al., 2011).

2. BACKGROUND

2.1. Chapter 1 "Abf1 is an Essential Protein that Participates in Cell Cycle Progression and Subtelomeric Silencing in *Candida glabrata*"

DNA replication and repair are crucial for survival in any living organism. The ARS-binding factor 1 (Abf1) plays an important role in DNA replication in *S. cerevisiae* and was first described as a general factor that binds to autonomously replicating sequences essential for the initiation of DNA replication. *Sc*Abf1 recruits the origin recognition complex (ORC) to ARS elements which allows the assembly of the pre-replication complex (pre-RC) that is a key step in the initiation of the DNA replication. Furthermore, the B3 element found at *ARS1* element is a binding site for Abf1 where it acts as a barrier, positioning the nucleosomes adjacent to the origin of replication. Also, *Scabf1* temperature sensitive alleles are defective in DNA replication (Reed et al., 1999). In addition, *Sc*Abf1 binds at the ARS found at *HMR* silent mating type locus required for transcriptional repression of the mating-type information (Abraham et al., 1984; Diffley and Stillman, 1988; Lipford and Bell, 2001). Another process important to correctly preserve the DNA, is the nucleotide excision repair (NER) machinery, where Rad7 and Rad16 proteins are key to this process. Abf1 has been shown to interact with Rad7 and Rad16 where it plays a role in NER.

Moreover, Abf1 transcriptionally regulates genes involved in a wide range of cellular processes including the regulation of carbon and nitrogen source utilization, sporulation, and meiosis (De Boer et al., 2000; Della Seta et al., 1990; Kovari and Cooper, 1991; Ozsarac et al., 1997; Rie Gailus-Durner et al., 1996; Trawick et al., 1992).

The structure of Abf1 is divided into two main regions the N-terminal domain that contains the zinc finger and the *trans* activation domains, and the C-terminal domain that is composed of two principal structures, both of which are essential. CS1 that consist of a NLS, and the CS2 that is responsible for the DNA replication, transcription, and remodeling functions (Miyake et al., 2002; Yarragudi et al., 2004). *C. glabrata* (*Nakaseomyces glabrata*) contains in its genome the orthologue gene for Abf1. In this work, we wished to characterized *Cg*Abf1 and determined its role

during the cell cycle progression and DNA replication, as well as its role in subtelomeric silencing at telomere E-R and other telomeres.

2.2. Chapter 2 "Negative regulation of adhesin-encoding genes requires Abf1 silencing factor"

Adhesion is a critical virulence trait in *C. glabrata*, which is the second most isolated *Candida* spp after *Candida albicans* in hospital infections, with a mortality rate of 30%. Our lab strain possesses a large battery of adhesin encoding genes that are mostly found in subtelomeric regions and subject to subtelomeric silencing. The principal adhesin that mediates adhesion to epithelial cells *in vitro* is Epa1, which is located at the telomere E-R and forms a cluster with *EPA2* and *EPA3*. These genes are negatively regulated by subtelomeric silencing, which depends on SIR complex, Rap1, Abf1 and yKu70/80, and is propagated from the telomere to the adjacent subtelomeric region (Castaño et al., 2005; De Las Peñas et al., 2003; Rosas-Hernández et al., 2008).

In addition, at the E-R subtelomere we previously identified different *cis*-acting elements which are crucial for the subtelomeric silencing mechanism. For example, the protosilencer Sil2126 located between *EPA3* and E-R telomere, can extend silencing from the telomere to a region ~20 Kb toward the centromere. Sil2126 has two important regions for its activity designated as R1 and R2. These regions contain binding sequences for the recruitment of Abf1 and Rap1 both proteins are essential for its function. Besides, Sil2126 depends on its orientation relative to the telomere as well as on its chromosomal context. Previous work has shown that Sil2126 can interact with the intergenic region between *EPA2* and *EPA3* remodeling the chromatin into a loop, repressing the expression of the genes inside this structure; also, additional structures can be formed between the flanking regions of *EPA1* and Sil2126 (Juárez-Reyes et al., 2012; López-Fuentes et al., 2018). An additional *cis*-acting element required for the negative regulation of *EPA1* is the Negative Element (NE) located in the *3'* intergenic region. Repression of P_{EPA1} takes place immediately after its activation when cells from SP are diluted in fresh media. This mechanism depends on yKu proteins and is independent of the subtelomeric silencing (Gallegos-García et al., 2012).

In this work, we wished to characterized the *cis*-acting elements in the intergenic regions between *EPA1* and *EPA2, EPA2* and *EPA3* and the upstream region of *EPA1*, all of which harbor putative binding sites for Abf1 and Rap1 and are important

for subtelomeric silencing by Sil2126. In addition, we investigated protein-protein interactions between silencing proteins to gain insight into how the spreading of protein complexes can remodel the shape of E-R chromosome and influence expression patterns of adhesins genes.

3. GENERAL AIM

To characterize the role of different silencing proteins in regulation of the expression of *EPA* genes at the E-R telomere in *Candida glabrata*.

3.1 Specific aims chapter 1

- To determine if Abf1 is essential for cell viability in *C. glabrata*.
- To determine if Abf1 has a role in subtelomeric silencing in *C. glabrata*.
- To determine if Abf1 participates in the cell cycle in *C. glabrata*.

3.2 Specific aims chapter 2

- To determine whether silencing proteins Abf1, Rap1, Sir3/4, yKu70/80 interact with each other.
- To determine if Abf1 and Rap1 are recruited at different positions throughout the promoter of *EPA1* and other *cis*-acting elements between *EPA1* and *EPA2* and *EPA2* and *EPA3*.
- To define the binding sequences recognized by Abf1 and Rap1 in *Candida glabrata*.
- To determine if Abf1 regulates the expression of different adhesins.

4. Materials and methods

4.1 Strains, plasmids, and primers

All strains, plasmids and primers used in this study are listed in tables S1, S2 and S3.

4.2 Media

Yeasts were grown in standard liquid media and for plates, 2% agar was added. Synthetic complete (SC) media contains: yeast nutrient base (YNB) without $(NH_4)_2SO_4$ or amino acids (1.7 g/L), $(NH_4)_2SO_4$ (5 g/L), casamino acids (CAA) (0.6%) and glucose (2%). Minimal media is equivalent to YNB without amino acids; 2% glucose (2%) and $(NH_4)_2SO_4$ (5 g/L) as nitrogen source. Rich medium (Yeast extract-peptone-dextrose or YPD) contains yeast extract (10 g/L), peptone (20 g/L), and glucose (2%). When necessary, YPD solid media was supplemented with nourseothricin (AG Scientific, San Diego, CA, USA) to 100 μg/mL and for liquid media to 50 μg/mL. Bacteria were grown in LB medium containing 5 g/L yeast extract, 10 g/L tryptone, 5 g/L NaCl and 1.5% agar was added for plates. All plasmids were transformed into *Escherichia coli* strain DH10 by electroporation and cells were plated onto LB with 100 μg/mL carbenicillin (AG Scientific, San Diego, CA, USA) for selection of plasmids. Yeast as well as bacteria were grown at 30ºC.

4.3 *C. glabrata* transformation

Yeast transformations with either supercoiled or digested plasmids were performed following the procedure described in (Castaño et al., 2003) using the LiOAc method.

4.4 *URA3* reporter insertions

We generated a collection of mutants that contain the reporter gene *URA3*, which, when expressed in the presence of the 5-FOA, this is converted into a toxic compound. In this way the level of silencing is proportional to the growth of the cells in media containing 5-FOA (Castaño et al., 2003). Strains with different *URA3* insertions were grown at 30ºC in YPD for 48 h to stationary phase. Serial, 10-fold dilutions were made in 96-well plates. Then, 5 μl of each dilution was spotted onto

SC-Ura, SC+5-FOA and YPD plates, after which plates were incubated for 48 h at 30ºC and photographed.

4.5 Co-immunoprecipitation assays

We constructed epitope-tagged versions of different silencing proteins, Rap1, Abf1, Sir3, Sir4, yKu70, and yKu80 were tagged with FLAG epitope at the C-terminal end and integrated at their respective native loci except for Abf1, where we constructed plasmid containing an N-terminal fusion with both FLAG and cMyc for *ABF1* under the inducible promoter P_{MT1} (pVA98 and pGH3). The tagged and control strains were cultivated in YPD and collected in stationary phase. Protein extraction and western blot assays were performed as described previously by(Orta-Zavalza et al., 2013) with certain modifications. In brief, cells were resuspended in lysis buffer (45 mM HEPES, 400 mM potassium acetate, 0.5% Nonidet P-40, 1 mM EDTA, 1 mM DTT, 1 mM PMSF, 1X complete protease inhibitors cocktail ROCHE®). To lyse the cells, we added 100 µl of zirconia beads, and lysed the cells using FastPrep®-24 (MP Biomedicals®) with the following settings: three sets of 60 s at 6 m/s and placing the lysates on ice five minutes in between. Then, the lysates were spun down at 14,500 rpm at 4 °C during 40 min, the supernatant was saved to calculate the protein concentration using the Bradford reagent. For each lysate, 100 µg of total protein was incubated at 4 °C for 1h with 30 µl of Sepharose beads coupled to protein G (SigmaBioSpec®). Samples were centrifuged at 14,500 rpm for five minutes at 4 °C and then transferred to a new tube. For immunoprecipitation, lysates were mixed with 50 µl of anti-FLAG or anti-cMyc agarose (Sigma®) and incubated at 4 °C for two hours while being inverted constantly. Supernatants and immunoprecipitates were collected by centrifugation, washed with Lysis buffer three times, and then resuspended in 40 µl of 2X SDS loading buffer and heated to 95ºC for five min. The input (20 µg of total protein), supernatant (1:20 of the immunoprecipitated extract) and the IPs were loaded onto a 10% SDS-polycrylamide gel. The proteins were blotted onto PVDF membranes (BIO-RAD®) and afterward incubated with anti-Flag (Sigma®) or anti-cMyc (Sigma®) antibodies for 2 h at room temperature. Excess of antibodies was washed and then the membrane was probed with a goat-anti-mouse

horseradish peroxidase-conjugated secondary antibody (MERC®). Signal was detected by Pierce® ECL Western Blotting Substrate (Thermo Scientific® 32106) and CL-XPosure films (Thermo Scientific® 34090).

4.6 Chromatin immunoprecipitation assays (ChIP-qPCR)

Chromatin was extracted as described in (López-Fuentes et al., 2018) with a few modifications. Briefly, 150 mL of yeast cultures in minimal medium were grown to an OD_{600nm} of 1 at 30 ºC with shaking. Cultures were put on ice for 15 min. Cells were fixed with formaldehyde to a final concentration of 1% during 15 min at 25ºC at 180 rpm. Cross-linking was achieved by the addition of 125 mM glycine and incubated for 5 min. Cells were collected and washed with Tris-Salt buffer [20 mM Tris-HCl (pH 7.5), 150 mM NaCl] twice and the supernatant was recovered into 1.5 mL tubes. Then, we lysed the cells with 500 μl of lysis buffer [10 mM EDTA (pH 8), 50 mM Tris-HCL (pH 8), 1% SDS and, 1 mM PSMF and the protease inhibitor ULTRA Tablet Mini/10 mL (EASYpack (ROCHE)] was added immediately before use. Then, cells were lysed by adding 500 μl glass beads and mixing thoroughly for 30 s and incubated on ice for one minute (this process was repeated 10 times). The chromatin obtained from the lysates was sheared by sonication with the following protocol: 30 cycles (total sonication time: 3 min 45 s) at 20% amplitude in Episonic multifunctional bioprocessor Model Oasis 180. We obtained DNA fragments of an average size ~500 bp. To immunoprecipitate the tagged proteins we used 5 μg mouse anti-FLAG (Sigma) or anti-cMyc (Millipore) coupled to Dynabeads Protein G for immunoprecipitation (Invitrogen). The immunoprecipitates with the Dynabeads were washed two times with Dilution buffer [20 mM Tris-HCl (pH 8), 2 mM EDTA (pH 8), 150 mM NaCl, 1% Triton] and washed for an additional four times with Wash buffer [20 mM Tris-HCl (pH 8), 2 mM EDTA (pH 8), 150 mM NaCl, 0.1% SDS, 1% Triton]. Protein and cross-linked DNA were eluted in 100 μl of Elution buffer [1% SDS, 0.1 M NaHCO3] and incubated at 65 ºC for 10 min. Crosslinking was reversed by incubating the mixture at 65 ºC overnight with 50 μg/ml proteinase K. DNA followed by phenol:chloroform:isoamyl alcohol mixture 25:24:1 (BioUltra, Sigma) extraction and precipitation with 5 M NaCl, glycogen and ethanol. Immunoprecipitates were

resuspended in 30 μl of TE [10 mM Tris-Cl (pH 8), 1 mM EDTA] with 2 μg/mL RNase cocktail (Ambion). To prepare Input DNA 20% of the sheared chromatin (after sonication) was mixed with 200 μl TE followed by DNA extraction as described previously. Both, the input and the immunoprecipitated DNA were used as templates for qPCR reactions performed with PikoReal Real-Time PCR System (Thermo Scientific) and SYBER Green PCR Master Mix (Invitrogen). The primers are listed in Table S3. For Rap1, the ChIP assays are presented as % input relative to *ISC1* binding and for Abf1 relative to binding to the telomere.

4.7 Identification of putative binding sites for Abf1 and Rap1 in *C. glabrata*

To identify the binding sites for Abf1 and Rap1 in *C. glabrata* frequency matrices were defined using the data base JASPAR (https://jaspar.genereg.net/search?q=&collection=CORE&tax_group=fungi) using *S. cerevisiae* as references due to the high percentage of identity between the DNA binding domains of both proteins. The *S. cerevisiae* matrices are the result of PBM, CSA, DIP-ChIP, and ChIP-EXO the accession numbers are: Abf1 MA0265.1 and MA0265.2, and for Rap1 MA03591.1 and MA0359.2. Using MEME suite, specifically the FIMO tool with the predetermined parameters (threshold *P* value: 0.001) and feeding the sequences obtained from the ChIP-qPCR that were enriched for each protein. As negative control we used a sequence in which we did not observe enrichment for either of these proteins. The results obtained were analyzed into matrices for *Cg*Abf1 and *Cg*Rap1 and graphed using the package Bioconductor for RStudio (https://bioconductor.org/packages/memes).

4.8 P_{EPA1} promoter activity using a GFP transcriptional fusion and analysis with FACS

Cells containing the transcriptional fusion of the *EPA1* promoter with GFP were grown in YPD media for 48 h at 30ºC, then diluted in fresh media to induce *EPA1* expression in CAA. Samples were taken every 2 h during an 8 h lapse and analyzed

by flow cytometry (FACS) using BD FACSCalibur Flow Cytometer with Cell Quest Pro software. The data was analyzed using GraphPad, PRISM.

4.9 Quantitative PCR (qPCR)

Total RNA was extracted as previously described in (Schmitt et al., 1990) with some modifications. Briefly, yeasts were inoculated at OD_{600nm} of 0.5 in 300 mL of YPD and incubated at 30 ºC with constant shaking (180 rpm) and samples of 50 mL were taken at 15, 30, 60 and 120 minutes. Harvested cells were centrifuged and resuspended in 1.2 mL of AE buffer (50 mM Sodium Acetate, 10 mM EDTA, pH 5.3). Then 40 μl of SDS 10% were added to 400 μl of resuspended cells and mixed with using vortex for two minutes, 500 μl of phenol saturated with citrate buffer 0.1 M (pH 4.3, P4682 Sigma) were added and mixed with vortex for two minutes, following an incubation of four minutes at 65 ºC and immediately frozen with liquid nitrogen and then defrosted at 25 ºC. Next, samples were centrifuged at 14,000 rpm during five minutes, the supernatant was recovered and 500 μl of phenol:chloroform:isoamyl alcohol mixture 25:24:1 (BioUltra, Sigma) were added and mixed with vortex for five minutes. Tubes were then centrifuged for 10 minutes at 14,000 rpm; then, the supernatant was transferred to a clean tube, and RNA was precipitated using sodium acetate (0.3 M pH 5.3) and molecular grade absolute ethanol. Afterwards, the precipitate was washed with 80% ethanol and the dried pellet resuspended in 20 μl of sterile water. The total RNA extracted was treated with DNase I (Invitrogen) to remove contaminating genomic DNA. cDNA synthesis was made using SuperScript II reverse transcriptase and the reverse primers for each gene. The reaction was performed at 42°C for 50 min. We used the Fast SYBR Green Master Mix (Applied Biosystems, Invitrogen) in a PikoReal 96 Real-Time PCR System (Thermo Scientific, USA) for the qPCR reaction. The internal control was *ACT1* for normalization and the threshold cycle ($2^{-\Delta\Delta Ct}$) method was used to calculate the differences in gene expression.

4.10 Adherence assays

Adherence assays were made as described by (Martínez-Jiménez et al. 2013). Briefly, yeast cells were grown to stationary phase (48 h) in YPD and then adjusted to an OD_{600nm} of 1.0 with Hanks Balanced Sal Solution (HBSS: 5.4 mM KCl, 0.3 mM Na_2HPO_4, 0.4 mM KH_2PO_4, 4.2 mM $NaHCO_3$, 0.6 $MgSO_4$, 137 mM NaCl, pH 7.4) and $CaCl_2$ (5 mM), 1 mL of the yeast cell suspension was added to each well of a 24 well plate containing fixed HeLa cells with 500 μl HBSS with $CaCl_2$. The plate was centrifuged at 1,000 rpm for 1 min. and incubated 1 hour at 25 ºC. Yeast adhered to HeLa monolayer after the washings were recovered adding 0.5 mL of wash buffer to each well (0.1% triton, 0.5% SDS, 10 mM EDTA, 1X PBS). Yeast cells were recovered by scraping off the well and resuspended in a 1.5 ml tube. Then, 10-fold serial dilutions were made in sterile water, 200 μl of each dilution was plated on YPD and incubated for 48 h at 30 ºC. CFUs of the recovered adherent yeast cells and input cells were counted. The percentage of adherence was calculated using the formula:

% Adherence = [CFU (adherent cells) / CFU (input cells)] * 100

4.11 Construction of Sir4, yKu70, and yKu80 fusions with YFP and mCherry

To visualize the distribution of the silencing proteins within the nuclei, we designed a cloning strategy using plasmids containing the epitopes pVA99 (P_{MT-1}::mCherry.*NAT*^{R}), pVA152 (P_{MT-1}::mCherry.*URA*+) and pVA87 (P_{MT-1}::*YFP*.*URA*+), where the expression of each gene cloned is under the control of the inducible promoter *MT-1*. We amplified the *HDF2*-ORF fragment (yKu80 1.848 Kb) with #3195 and #3196 primers and digested *Cla*I/*Sal*I enzymes and clone into pVA87 (pGH24) and pVA152 (pGH25). In a similar manner we amplified the *NUP49*-ORF (nuclear periphery protein) with #3191 and #3192 primers (PCR fragment of 1.515 Kb) and digested with *Sal*I/*Xho*I and cloned into pVA99 (pGH27). Plasmids obtained were transformed by electroporation using DH10 cells. Then the plasmids with these fusions were transformed into different genetic backgrounds of *C. glabrata* as previously described.

4.12 Fluorescence microscopy

Strains with the different fluorescent epitopes were grown 24 h in SC-Ura at 30ºC, then diluted in 5 mL fresh media during 2 h at 30ºC. One mL samples were taken from each strain and washed with 1 mL of sterile MilliQ water, washed cells were resuspended in 100 μl of MilliQ water and 5 μl of the resuspended cells were analyzed in the Axio Imager.m2 (Carl Zeiss). Images obtained were analyzed using the software AxioVision v.4.8.2.9 image browser.

5. Results

Chapter 1. Abf1 is an Essential Protein that Participates in Cell Cycle Progression and Subtelomeric Silencing in *Candida glabrata*

Journal of *Fungi*

MDPI

Article

Abf1 Is an Essential Protein That Participates in Cell Cycle Progression and Subtelomeric Silencing in *Candida glabrata*

Grecia Hernández-Hernández [1], Laura A. Vera-Salazar [1], Leonardo Castanedo [2], Eunice López-Fuentes [3], Guadalupe Gutiérrez-Escobedo [1], Alejandro De Las Peñas [1] and Irene Castaño [1,*]

[1] División de Biología Molecular, Instituto Potosino de Investigación Científica y Tecnológica (IPICYT), Camino a la Presa San José No. 2055 Col. Lomas 4 Sección, San Luis Potosí CP 78233, Mexico; grecia.hernandez@ipicyt.edu.mx (G.H.-H.); laura.vera@ipicyt.edu.mx (L.A.V.-S.); maria.gutierrez@ipicyt.edu.mx (G.G.-E.); cano@ipicyt.edu.mx (A.D.L.P.)

[2] Department of Plant Physiology, Faculty of Biology and Biotechnology, Ruhr University Bochum, Universitätsstrasse, 150 ND3/30, D-44801 Bochum, Germany; castanedo.leonardo@gmail.com

[3] Division of Hematology and Oncology, Department of Pediatrics, University of California, San Francisco, CA 94158, USA; eunice.lopezfuentes@ucsf.edu

* Correspondence: icastano@ipicyt.edu.mx; Tel.: +52-444-834-2038

Abstract: Accurate DNA replication and segregation is key to reproduction and cell viability in all organisms. Autonomously replicating sequence-binding factor 1 (Abf1) is a multifunctional protein that has essential roles in replication, transcription, and regional silencing in the model yeast *Saccharomyces cerevisiae*. In the opportunistic pathogenic fungus *Candida glabrata*, which is closely related to *S. cerevisiae*, these processes are important for survival within the host, for example, the regulation of transcription of virulence-related genes like those involved in adherence. Here, we describe that *CgABF1* is an essential gene required for cell viability and silencing near the telomeres, where many adhesin-encoding genes reside. *Cg*Abf1 mediated subtelomeric silencing depends on the 43 C-terminal amino acids. We also found that abnormal expression, depletion, or overexpression of Abf1, results in defects in nuclear morphology, nuclear segregation, and transit through the cell cycle. In the absence of *ABF1*, cells are arrested in G2 but start cycling again after 9 h, coinciding with the loss of cell viability and the appearance of cells with higher DNA content. Overexpression of *CgABF1* causes defects in nuclear segregation and cell cycle progression. We suggest that these effects could be due to the deregulation of DNA replication.

Keywords: *Candida glabrata*; Abf1; DNA replication; cell cycle; subtelomeric silencing

check for updates

Citation: Hernández-Hernández, G.; Vera-Salazar, L.A.; Castanedo, L.; López-Fuentes, E.; Gutiérrez-Escobedo, G.; De Las Peñas, A.; Castaño, I. Abf1 Is an Essential Protein That Participates in Cell Cycle Progression and Subtelomeric Silencing in *Candida glabrata*. *J. Fungi* **2021**, *7*, 1005. https://doi.org/10.3390/jof7121005

Academic Editors: Germán Larriba and Toni Ciudad

Chapter 2. Abf1 negatively regulates the expression of adhesin encoding genes in *Candida glabrata*

Grecia Hernández-Hernández[1], Laura A. Vera-Salazar[1], Guadalupe Gutiérrez-Escobedo[1], Nicolás Gómez-Hernández[1], Osney Leiva- Peláez[1], Alejandro De Las Peñas[1] and Irene Castaño[1]*

[1]División de Biología Molecular, Instituto Potosino de Investigación Científica y Tecnológica, Camino a la Presa San José, #2055, Col. Lomas 4ª sección. San Luis Potosí, San Luis Potosí 78216, México.

*Corresponding autor. E-mail: icastano@ipicyt.edu.mx, Tel. (52) 444 834 2038

Abstract

Adherence is a major virulence trait in *Candida glabrata* that in many strains depends on the *EPA* (Epithelial Adhesion) genes, which confer the ability to adhere to the epithelial cells of the host. The *EPA* genes are generally found at subtelomeric regions which results in subtelomeric silencing of their transcription. In *C. glabrata*, subtelomeric silencing depends on different protein complexes like SIR, yKu complexes and other proteins like Rap1 and Abf1. At the *EPA1* locus, which encodes the main adhesin Epa1, we previously found at least two *cis*-acting elements, the protosilencer Sil2126 and the negative element (NE), that contribute to the propagation of silencing from the telomere to the subtelomeric region. In this work, using ChIP-qPCR, we found that Abf1 predominantly binds to the *EPA1* promoter region leading to negative regulation of *EPA1* expression. Moreover, the mutant *abf1-43*, which lacks the last 43 amino acids at its C-terminal, and is defective for subtelomeric silencing, exhibits hyperadherence to epithelial cells *in vitro* in comparison to the parental strain, suggesting that *EPA1* is derepressed. Also, we determined the motif binding sequences for Abf1 and Rap1 in *C. glabrata*, using the data from the ChIP assays.

Key words: Abf1, subtelomeric silencing, adhesins, *EPA1*.

Introduction

Genetic and phenotypic variability plays an important role in the adaptation of the organisms to their environmental conditions. Several human pathogens can shape the gene expression patterns to successfully initiate an infection in the host (Helmstetter et al., 2022). Such is the case of *Candida glabrata*, which is normally part of the healthy microbiota of humans, but when the immune system is compromised it can cause disease, as it possesses different mechanisms to succeed as a pathogen such as its ability to adhere to different biotic and abiotic surfaces. *C. glabrata* harbors a broad battery of genes encoding cell wall proteins that play an important role in adhesion. The largest family of adhesins is the EPA family of which Epa1 is the founding member (Cormack et al., 1999a; De Groot et al., 2008; Xu et al., 2020). In the BG14 laboratory strain of *C. glabrata*, Epa1, encoded by the *EPA1* gene, mediates most of the adhesion to epithelial cells *in vitro*. *EPA1* gene is located at the right subtelomeric region of chromosome E (telomere E-R) where it forms a cluster with two other adhesins *EPA2* and *EPA3* (De Las Peñas et al., 2003). The expression of *EPA1* is regulated at least by two different mechanisms, the first involves the activation of transcription after dilution of stationary phase (SP) cells into fresh media, in which *EPA1* is rapidly induced and immediately after, transcription is repressed during log phase. This repression involves the *cis*-acting element called the negative element (NE) found at the 3' intergenic region of *EPA1* and depends on the protein complex yKu formed by yKu70/80 but is independent of the silencing from the telomere (Gallegos-García et al., 2012a). The second mechanism is the subtelomeric silencing, controlled in *C. glabrata* primarily by the SIR complex (Silent Information Regulator) formed by Sir2, Sir3, and Sir4, and the silencing propagates from the telomere to the subtelomere and represses the genes found in this region (Castaño et al., 2005). Other proteins involved in subtelomeric silencing in *C. glabrata* are the yKu complex which participates at different levels depending on the subtelomeric region, Rap1 (Repressor/activator protein 1) that is found at the telomere repeats in *C. glabrata*, and Abf1, an essential protein that has multiple roles and binds directly to the Autonomous Replicating Sequence (ARS) having a crucial role in the initiation of DNA replication, other process that involve Abf1 are DNA repair, activation and

repression of transcription in the non-pathogenic, closely related yeast *Saccharomyces cerevisiae* and in *C. glabrata* (De Las Peñas et al., 2003; Hernández-Hernández et al., 2021; Miyake et al., 2002; Rhode et al., 1989b; Rosas-Hernández et al., 2008). Interestingly, although most of the *EPA* genes expression is controlled by subtelomeric silencing, many of them exhibit a differential expression pattern under various conditions. For instance, *EPA2* is induced in the presence of oxidative stress and depends on the transcription factors Yap1 and Skn7 (Juárez-Cepeda et al., 2015a), and *EPA3* is differentially expressed in biofilms only in planktonic cells (Kraneveld et al., 2011).

We previously identified a *cis*-acting element at the E-R telomere called Sil2126, a protosilencer located between *EPA3* and the telomere. This element can propagate the silencing of a reporter gene when inserted distally from the telomere (31.5 Kb), a distance where there is normally no silencing (Juárez-Reyes et al., 2012). Moreover, previous data shows that the activity of Sil2126 depends on the E-R telomere context specifically, since there are other *cis*-acting elements in the *EPA2-EPA3* intergenic region. Sil2126 also requires *trans*-acting elements such as the SIR complex, Rap1, Rif1, and Abf1 (Hernández-Hernández et al., 2021; López-Fuentes et al., 2018). We also found that Sil2126 can interact with *EPA2-EPA3* intergenic region through a DNA loop where protein-protein interactions are required to remodel the three-dimensional structure of the telomere E-R. In addition, alternative structures can be formed between Sil2126 with other intergenic regions in the E-R subtelomere, for example interactions can be detected by 3-C experiments between Sil2126 and the intergenic regions between *EPA1* and *EPA2* or *HYR1* and *EPA1*. These interactions were less frequent that the ones observed with the *EPA2- EPA3* intergenic region, which suggests that these structures are dynamic and respond to different stimuli to fully repress or activate the genes found at the E-R subtelomere (López-Fuentes et al., 2018).

Here, we show by ChIP-qPCR that Abf1 binds most efficiently to the *EPA1* promoter region and to the *EPA1 – EPA2* intergenic region where the *cis*-acting NE is located, albeit less efficiently. With this data we generated putative *C. glabrata* Rap1 and Abf1 consensus binding sequences and a more detailed map of Abf1 and Rap1 putative binding sites throughout the E-R telomere. Furthermore, we showed that

Abf1 is required for *EPA1* repression and that in the strain containing the truncated allele Abf1-43, defective in subtelomeric silencing, results in an increase in adherence to epithelial cells *in vitro*.

Results

Subtelomeric silencing at chromosome E-R of *C. glabrata* does not extend beyond the *EPA1* promoter.

To define whether the 5' intergenic region of *EPA1* is subject to subtelomeric silencing we designed a series of insertional mutants using the reporter gene *URA3* at different distances from the start of the *EPA1* transcription site. The first insertion is located just before the ATG codon of *EPA1* (at -1 from *EPA1*) and it is moderately silenced, as measured by the moderate ability of the strain to grow on 5-FOA media, which is toxic to cells expressing the *URA3* reporter gene. The second insertion at -0.791 Kb from *EPA1* (-26.7 Kb from the telomere) and, the third insertion is located at -2.2 Kb from *EPA1* start codon which corresponds to -28.2 Kb from the telomere. We found that these last two insertions are not silenced since there is no growth on 5-FOA containing plates. This indicates that silencing does not extend over 26.5 Kb from the E-R telomere (Fig. 1).

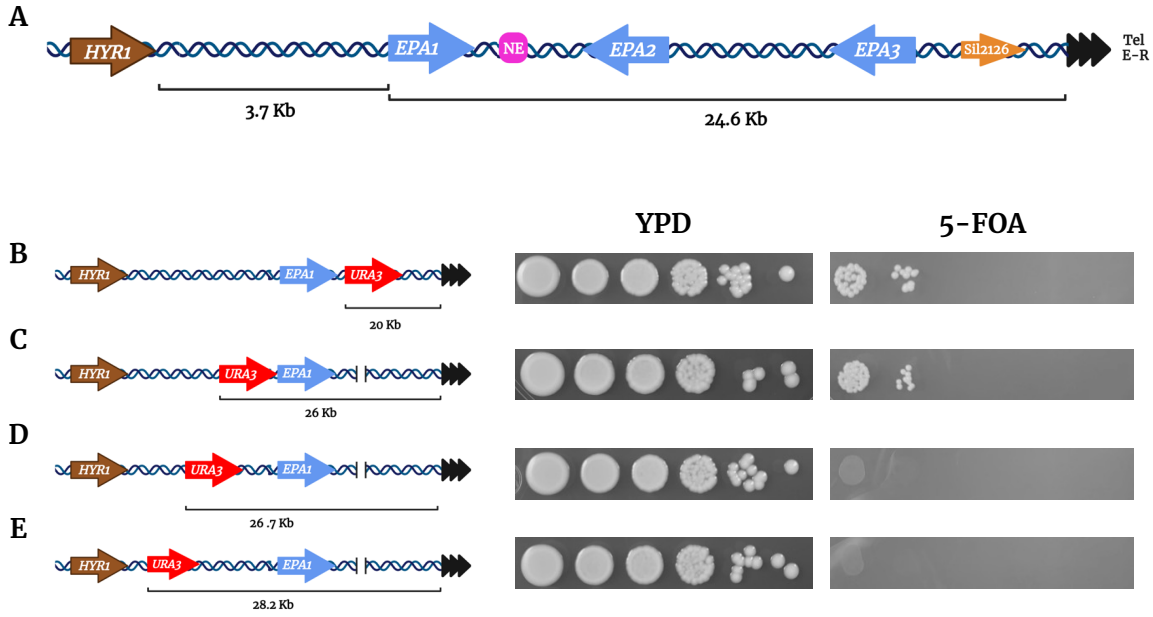

Fig. 1 Subtelomeric silencing in *C. glabrata* extends to ~ 20 Kb at telomere E-R. A) Schematic representation of telomere E-R, where *EPA1, EPA2,* and *EPA3* are located. B-E) Schematic representation of the intergenic region between *HYR1* and *EPA1* at Tel E-R;. the red arrows represent the position of insertions of the *URA3* reporter, and the distance from the telomere is indicated below each insertion. 5 µl of ten-fold serial dilutions of cells grown to stationary phase were spotted onto the media indicated, incubated at 30ºC for 48 h, and then photographed.

Abf1 and Rap1 bind to different *cis*-acting elements in the *EPA1-2*, and *EPA2-3* intergenic regions

We have found several putative binding sites for Abf1 and Rap1 silencing proteins in the subtelomeric region E-R in our standard strain BG14, where the cluster formed by *EPA1*, *EPA2*, and *EPA3* genes are located. Abf1 and Rap1 are required for subtelomeric silencing mediated by Sil2126, which has functional binding sites for these proteins. Additionally, Sil2126 requires other uncharacterized *cis*-acting elements in the intergenic region between *EPA2* and *EPA3* when the protosilencer is removed from its original position near the telomere and inserted 32 Kb away from it (Sil@-32) (Juárez-Reyes et al., 2012; López-Fuentes et al., 2018). We determined whether Abf1 and Rap1 bind to uncharacterized *cis*-acting elements in these regions by ChIP-qPCR. We found that Abf1 and Rap1 are enriched at the promoter region of *EPA2*, Rap1 binds with higher efficiency to the region ~ 2 Kb upstream of the ATG of *EPA2* whereas Abf1 binds further upstream of the initiation codon of *EPA2* (Fig. 2B). We also analyzed the intergenic region between *EPA1* and *EPA2*, where the *cis*-acting element NE is located. We found that Abf1 binding is increased within or immediately downstream of the NE. In contrast, Rap1 is not enriched in this region in the parental BG14 strain (Fig. 2C).

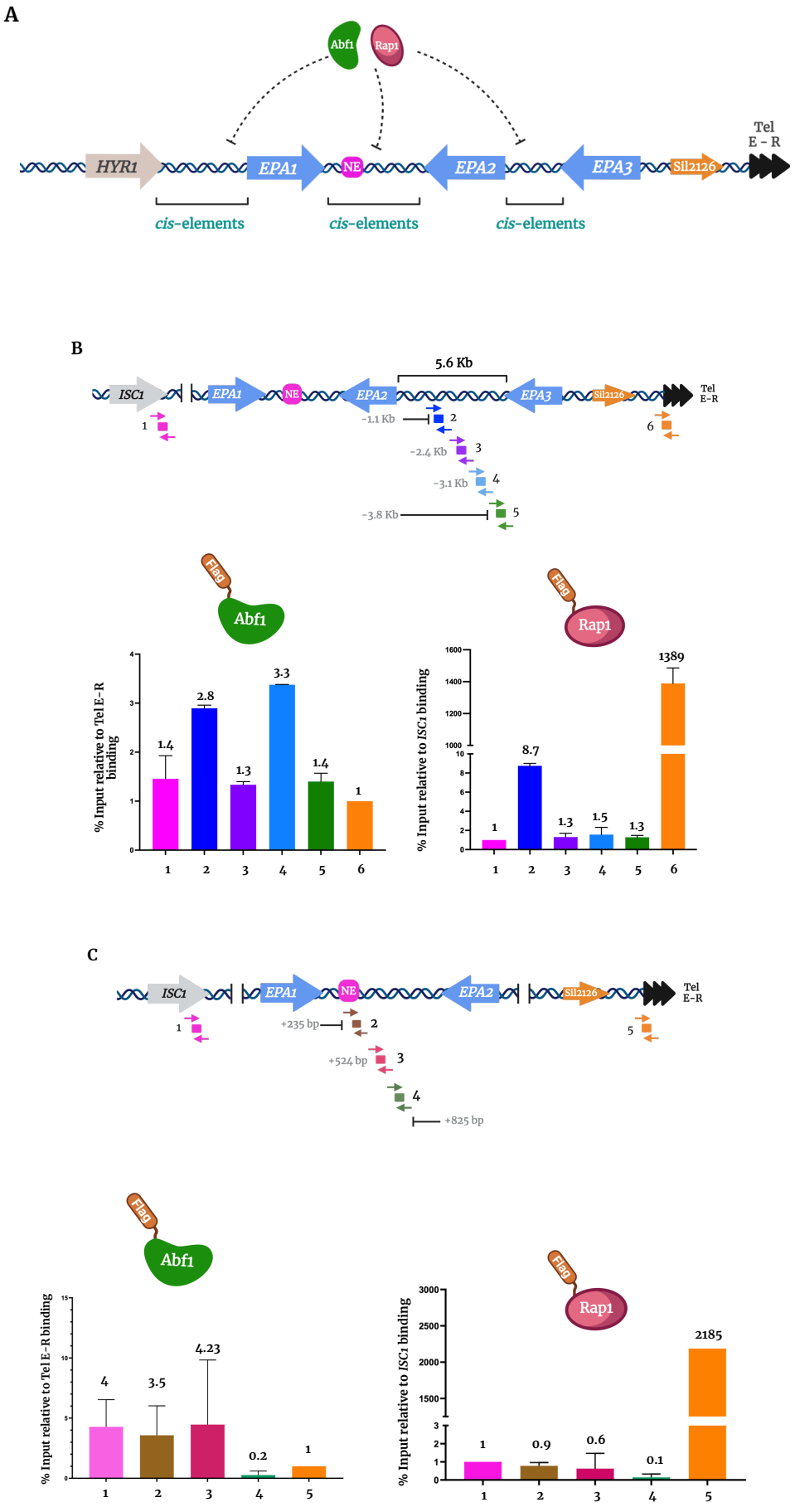
A
Abf1
Rap1
HYR1
EPA1
NE
EPA2
EPA3
Sil2126
Tel
E - R
cis-elements
cis-elements
cis-elements
B
5.6 Kb
ISC1
EPA1
NE
EPA2
EPA3
Sil2126
Tel
E-R
-1.1 Kb
-2.4 Kb
-3.1 Kb
-3.8 Kb
Flag
Abf1
% Input relative to Tel E-R binding
1.4
2.8
1.3
3.3
1.4
1
Flag
Rap1
% Input relative to ISC1 binding
1
8.7
1.3
1.5
1.3
1389
C
ISC1
EPA1
NE
EPA2
Sil2126
Tel
E-R
+235 bp
+524 bp
+825 bp
Flag
Abf1
% Input relative to Tel E-R binding
4
3.5
4.23
0.2
1
Flag
Rap1
% Input relative to ISC1 binding
1
0.9
0.6
0.1
2185

Fig. 2 Abf1 and Rap1 bind to different positions throughout the telomere E-R. A) Schematic representation of uncharacterized *cis*-acting elements at telomere E-R, that contain putative binding sites for Abf1 and Rap1 (López-Fuentes et al., 2018b). B) top: Schematic representation of the intergenic region between *EPA2* and EPA3 at telomere E-R. The position of the amplified fragments in the ChIP-qPCR are represented by the color bars below the map, numbered from 1 to 6. Bottom left: graph corresponds to the enrichment of Abf1, calculated as enrichment relative to the enrichment at the telomere E-R (where Abf1 does not bind, oligo pair 6). Bottom right: graph corresponds to Rap1 enrichment calculated as binding relative to *ISC1* (where Rap1 does not bind, oligo pair 1). C) Top: schematic representation of the intergenic region between *EPA1*-*EPA2*. The position of the amplified fragments in the ChIP-qPCR are represented by the color bars below the scheme, numbered from 1 to 5. Bottom left: graph shows the enrichment of Abf1, calculated as the enrichment relative to the enrichment at the telomere E-R (where Abf1 does not bind, oligo pair 6). Bottom right: graph shows Rap1 enrichment calculated as binding relative to *ISC1* (where Rap1 does not bind, oligo pair 1). Statistical analysis was performed using an unpaired two tailed Student's t-test with $P < 0.001$.

Abf1 binds to the promoter region of *EPA1*

Since Sil2126 can interact with the intergenic regions flanking *EPA1* (López-Fuentes et al., 2018), we analyzed the promoter region of *EPA1* for *cis*-acting elements that could recruit Abf1 and Rap1. The results showed that Abf1 is enriched in at least two points upstream *EPA1* centered at ~2 Kb upstream of the *EPA1* initiation codon. In comparison, Rap1 was not enriched in this region (Fig. 3). These data could suggest that Abf1 binding at this region represses the transcription of *EPA1*.

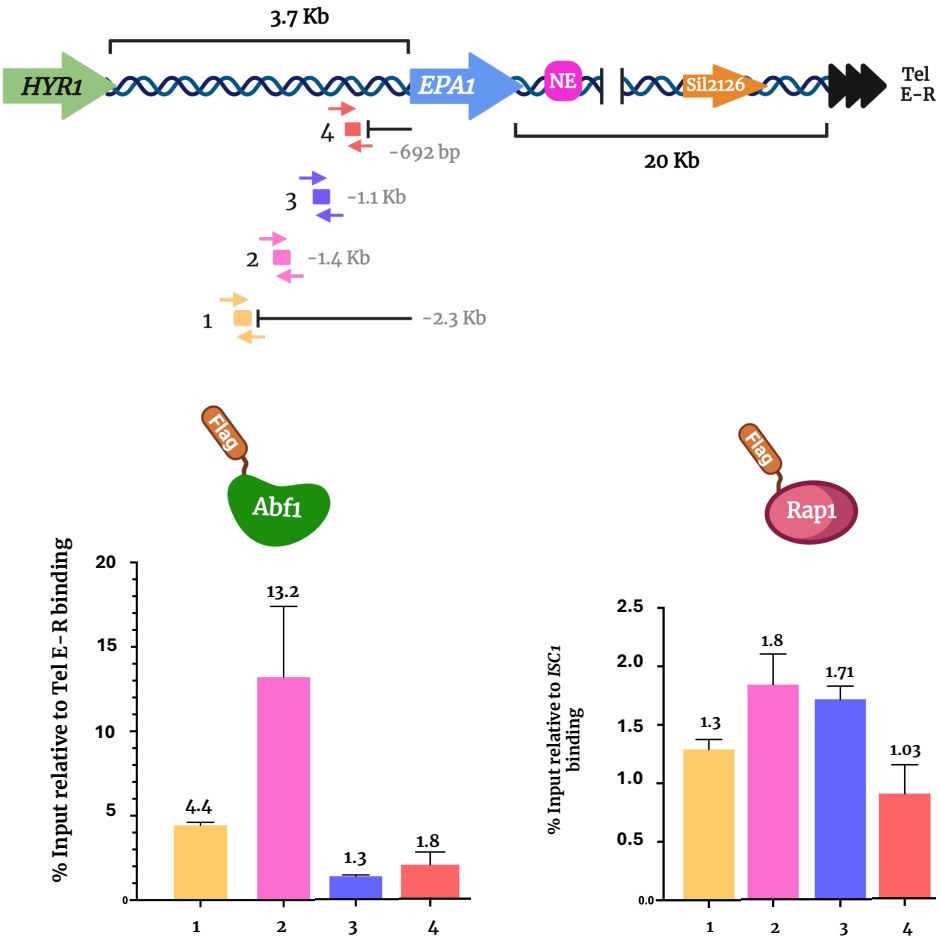

Fig. 3 Abf1 and Rap1 bind to the promoter region of *EPA1*. Schematic representation of the promoter region of *EPA1*. Position of the amplified fragments with the shown oligonucleotides pairs in the ChIP-qPCR are represented by the color bars below the scheme, numbered from 1 to 4 (top). From left to right enrichment for Abf1 was calculated as binding relative to the telomere E-R. Rap1 enrichment was calculated as binding relative to *ISC1* as indicated for Figure 2.

Abf1 represses the expression of *EPA1* in *C. glabrata*

We next decided to determine whether a silencing deficient, truncated version of Abf1 which lacks the last 43 amino acids at the C-terminus of Abf1, results in increased expression of *EPA1*. Because Abf1 is an essential gene in *C. glabrata* we evaluated a truncated allele *abf1-43* which lacks the last 43 amino acids and is defective for silencing without compromising cell viability (Hernández-Hernández et al., 2021).

RNA was isolated from the parental strain and *abf1-43* mutant, from samples taken from SP, 30, 60, and 120 minutes after dilution into fresh media. Expression of *EPA1* in SP for both strains is null, as previously described in (Castaño et al., 2005), but in early logarithmic phase (30 min after dilution into fresh media), *EPA1* is strongly induced, in the *abf1-43* we observed at least 10 times more *EPA1* expression than in the parental strain, this difference is increased over time up to 120 min. Altogether, these data support that binding of Abf1 to the regulatory region of *EPA1*, represses its expression (Fig. 4A).

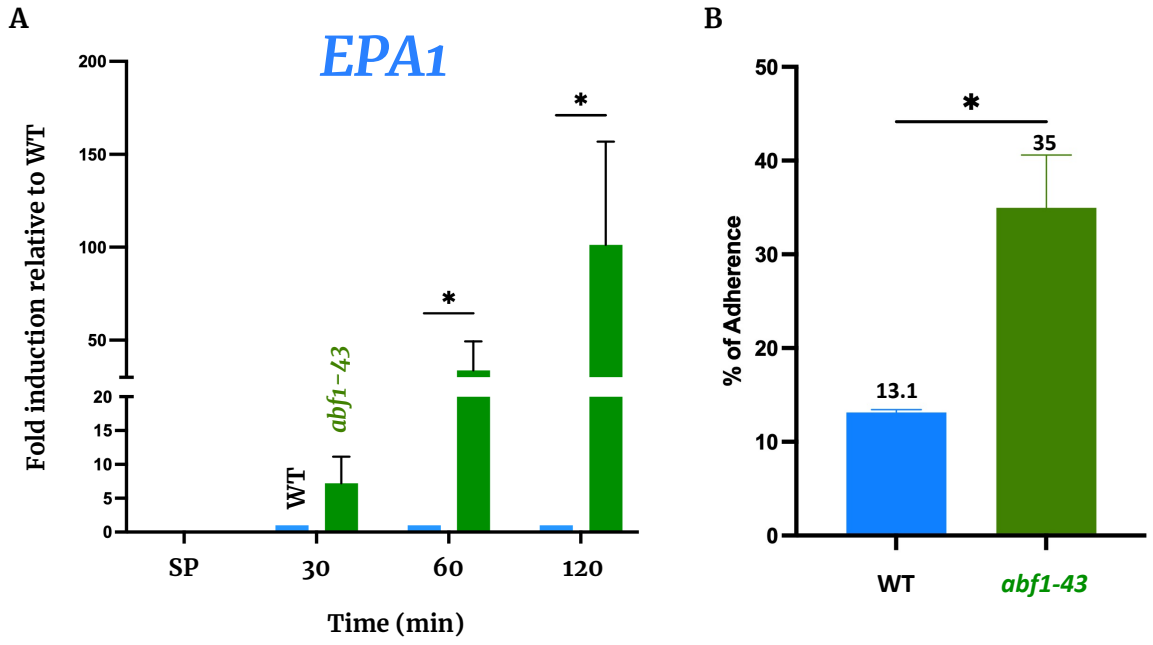

Fig. 4 Abf1 represses *EPA1* expression. A) In the *abf1-43* mutant *EPA1* expression increases in early log phase in comparison to the parental strain. Stationary phase cells of *C. glabrata* (BG14) and *abf1-43* mutant were grown for 48 h at 30ºC with constant shaking in YPD, then diluted in fresh media and adjusted to an OD_{600} of 0.5 and then grown for 2 h, samples were taken at 30, 60 and 120 min after dilution into fresh media. Total RNA was extracted and used for qPCR (See Material and Methods). Results are expressed as relative expression to *ACT1* and normalized to the parental strain under

the same conditions. Three biological replicates and two technical experiments were carried out. Statistical analysis was performed using two-way ANOVA (alpha < 0.05). B) In the *abf1-43* background, adhesion to epithelial cells *in vitro* is increased. Percentage of adhesion was calculated as the percentage of cells from the stationary phase (input) relative to the percentage that remain adhered to a monolayer of HeLa cells after washing cells that did not adhere. Blue bar corresponds to the percentage of adherence from the parental strain, green bar corresponds to the percentage of adherence of the truncated allele *abf1-43*. Data represent the mean of three independent biological replicates. Statistical analysis was performed using *t*-test ($P < 0.05$).

Silencing defective *abf1-43* mutant is more adherent to epithelial cells *in vitro*

Because the *abf1-43* strain shows a significant induction of *EPA1* immediately after dilution of SP cells into fresh media, we decided to determine whether this strain displays increased adhesion to HeLa epithelial cells *in vitro* in SP cells where *EPA1* is not induced. Cells from stationary phase (SP) of the parental strain and the *abf1-43* mutant were incubated with a monolayer of HeLa cells and the cells that did not adhere to the epithelial cells were washed off and the adherent cells were recovered and CFUs were determined. The results show that 35% of the *abf1-43* cells were adherent to epithelial cells in comparison with 13% of the parental strain under these conditions (Fig. 4B). These data support the idea that Abf1 binding to the promoter of *EPA1* plays a negative role in the expression of *EPA1* and in consequence, in the ability to adhere to epithelial cells.

Abf1 and Rap1 consensus binding sequences at the telomere E-R of *C. glabrata* are very similar to the corresponding recognition sites in *S. cerevisiae*

The consensus sequences recognized by Rap1 and Abf1 of *C. glabrata* have not yet been described. The putative DNA binding domains of *C. glabrata*'s Abf1 and Rap1 are well conserved with the orthologous *S. cerevisiae* Rap1 and Abf1 domains, (*Sc*Abf1 vs. *Cg*Abf1 65% identity, *Sc*Rap1 vs. *Cg*Rap1, 73%identity) (Hernández-Hernández et al., 2021).

Our sequence analysis from the ChIP data from the regions evaluated at the telomere E-R exhibit similarities in the core sequences recognized by both *Cg*Abf1 and. *Sc*Abf1, as well as *Cg*Rap1 vs. *Sc*Rap1 (Fig. 5B-C). We defined two frequency matrices for *Cg*Abf1 and *Cg*Rap1and found that *Cg*Rap1 binding sequences are less variable that the ones for *Sc*Rap1, this might be due to the limited region that we evaluated where *Cg*Rap1 is primarily enriched at the tandem repeats at telomere

(Fig. 5A, C). On the other hand, for *Cg*Abf1 we found both frequency matrices are also less variable than *Sc*Abf1 but are highly similar in key base pairs at the beginning and the end of both consensus sequences (Fig. 5B). Also, these matrices are not much different with each other in the case for the Autonomous Replication Sequence (ARS) and the silencing sequences where both are required for Abf1 binding.

It's worth noticing that the reference matrices come from much more deep sequencing assays, most from whole genome sequencing analysis in *S. cerevisiae*, which might account for the higher variability in comparison to the ones that we characterized at the telomere E-R.

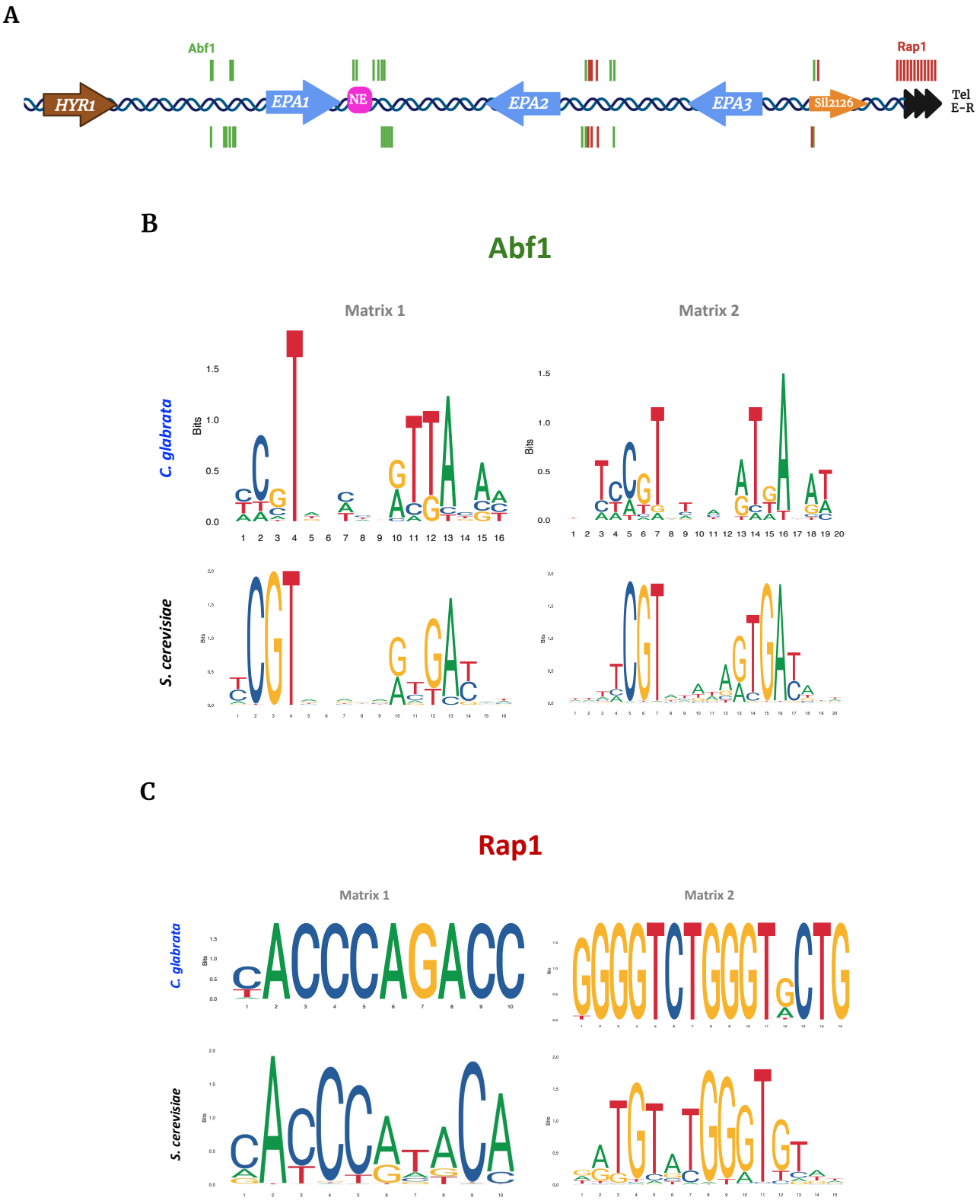

Fig. 5 Consensus DNA binding sequences for Abf1 and Rap1 in *C. glabrata* at tel E-R. A) Schematic representation of the binding sites for Abf1 and Rap1 at Tel E-R obtained from ChIP-qPCR data, using FIMO tool from the MEME Suite server. B) Binding sequences obtained for Abf1 in *C. glabrata* (top) in comparison to the binding sites for *S.*

cerevisiae (bottom). C) Binding sequences obtained for Rap1 in *C. glabrata* (top) in comparison to the binding sites for *S. cerevisiae* (bottom).

6. Additional results

6.1. Abf1 contributes to the induction of *EPA1* promoter in logarithmic phase in a NE dependant manner.

To evaluate *EPA1* expression in the context of the telomere in the *abf1-43* background, we used a transcriptional fusion of *EPA1* promoter with *GFP* and measured activity of the promoter by flow cytometry in three different backgrounds: 1) P_{EPA1}::*GFP* carrying an insertion of 3.797 Kb (pYiplac211 plasmid) 300 bp downstream the stop codon of Epa1, which increases the distance between *EPA1* and the NE, 2) P_{EPA1}::*GFP* where Sil2126 and NE are located at their original position in the chromosome, and 3) P_{EPA1}::*GFP* where Sil2126 was inserted 32 Kb from the telomere (Sil@-32 Kb) (Fig. 8). We previously described that P_{EPA1} is rapidly induced upon dilution of stationary phase (SP) cells into fresh media (Gallegos-García et al., 2012), therefore, we used the SP cells and diluted them into fresh media and measured GFP fluorescence every two hours during 8 h. The results are shown in Fig. 8. In strain 1 which carries the *abf1-43* allele, there is a reduced induction of GFP upon dilution of SP cells into fresh media in comparison to the *ABF1+* strain. After 4 h, there is a similar repression of P_{ABF1} in *ABF1+* and *abf1-43* strains. In strain 2, we observed no induction in *abf1-43* compared to a 4.3-fold induction of the promoter in the *ABF1+* strain, but this difference was not statistically significant. We observed no activity of the promoter in strain 3 either. Our data suggest that Abf1 might play a small role in the induction of P_{EPA1} in certain conditions for short periods of time.

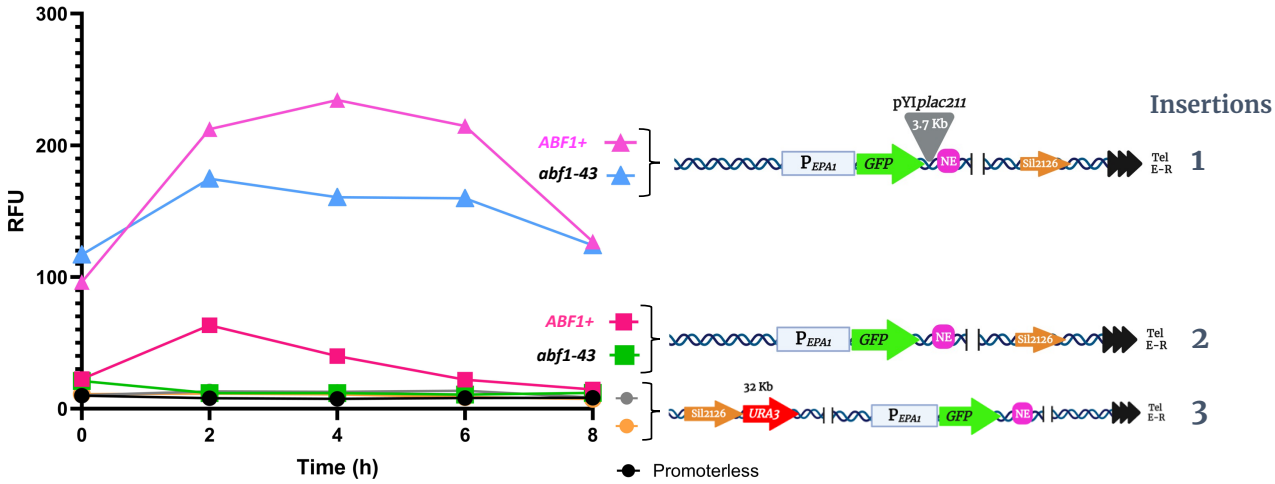

Strain	Fold induction (2 h)
P_{EPA1}:*GFP* pYlplac211 (*ABF1+*)	2.2
P_{EPA1}:*GFP* pYlplac211 (*abf1-43*)	1.6
P_{EPA1}:*GFP* (*ABF1+*)	2.6

Figure 8 *abf1-43* has a negative effect on the induction of the promoter *EPA1*. Strains used were grown 48 h at 30º in rich media (YPD), then diluted in fresh media adjusted at OD_{600} 0.5, samples were taken every 2 h and measure P_{EPA1}::GFP activity in FACS.

6.2. Abf1 binds to its own promoter region.

Since Sc*ABF1* has been shown to regulate its own synthesis, we analyzed *in silico* with JASPAR server the upstream and downstream regions of *CgABF1* (Chr J-R) to look for *Cg*Abf1 binding sites (Fig. 9A). We found few putative binding sites at the flanking intergenic regions of *CgABF1*. We then used ChIP-qPCR with Flag-Abf1 driven by P_{MT-1} (López-Fuentes et al., 2018) and found that Abf1 is enriched upstream of *ABF1* with a relative frequency of 22% (Fig. 9B). These data are consistent with the notion that Abf1 might indeed play a role in the regulation of its own transcription. We also looked for Rap1 binding sites in the *CgRAP1* flanking intergenic regions, but we did not observe enrichment of *Cg*Rap1 at the upstream region of *CgRAP1* (Fig. 9B).

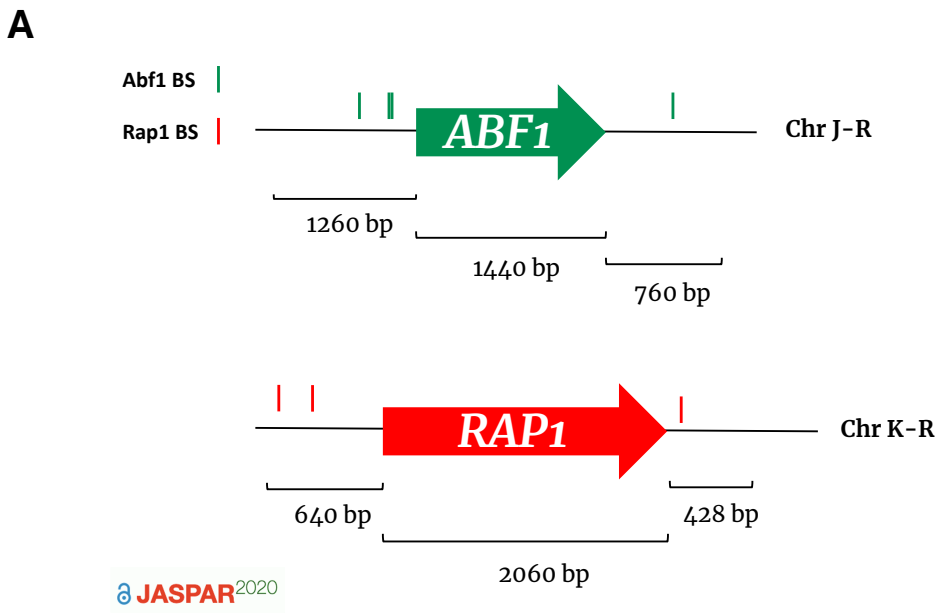

Fornes O, *et al. Nucleic Acids Res.* (2019)

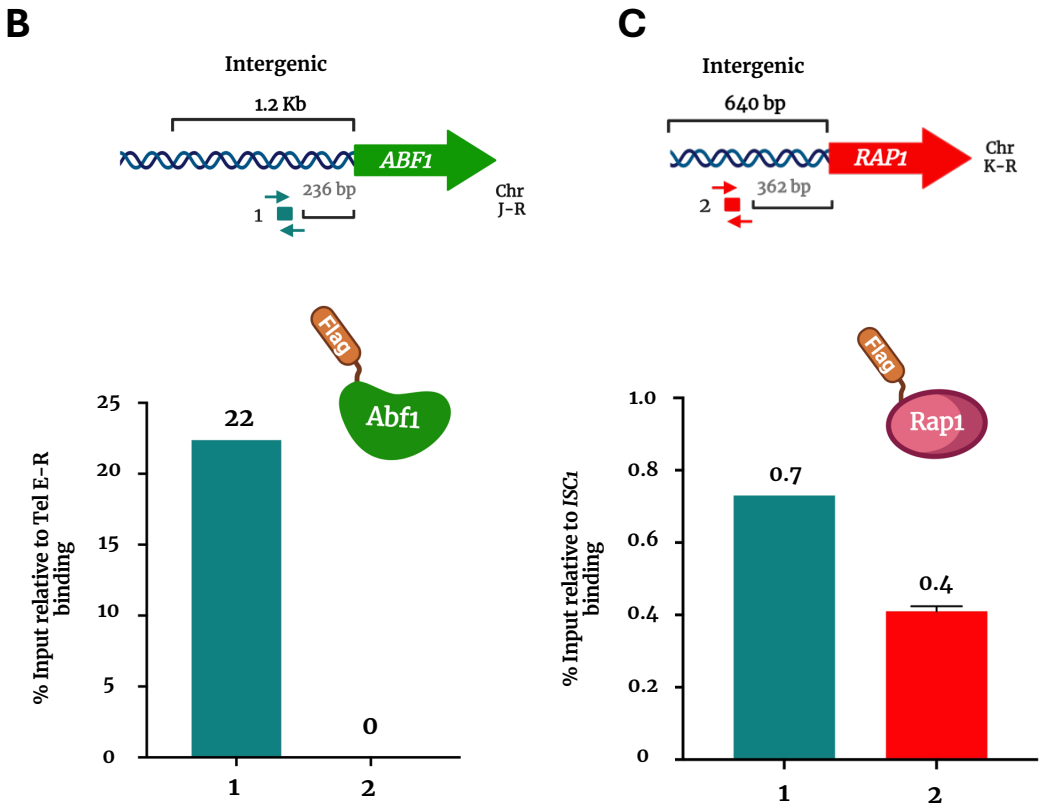

Figure 9 Abf1, but not Rap1 binds to its own promoter in *C. glabrata*. A; Schematic representation of the binding sites for Abf1 and Rap1 at their own intergenic regions in *C. glabrata*. Green lines represent the putative binding sites for Abf1, red lines represent putative binding sites for Rap1. Binding sites were determined with the JASPAR 2020 server, using the consensus sequence for *Sc*Abf1 and *Sc*Rap1. B; percentage of enrichment relative to the telomere for Flag-*Cg*Abf1. C; percentage of enrichment relative to *ISC1* for *Cg*Rap1-Flag.

6.3. Silencing proteins form a complex in *C. glabrata.*

Because Rap1 and Abf1 are abundantly enriched along the telomere E-R, the protosilencer Sil2126 at is original position and when inserted at -32 Kb (López-Fuentes et al., 2018), it suggests that Sil2126 recruits Abf1 and Rap1 to start the nucleation of other silencing proteins such as SIR complex that triggers the spreading of silent chromatin. Therefore, we decided to assess if some of the silencing proteins can interact with each other using CoIP assays. The results show that Abf1 can interact with several silencing proteins like Rap1, Sir3/4, and yKu70/80 (Fig. 10); this suggests that protein-protein interactions also play an important role in establishment and spreading of silencing at the subtelomeric region.

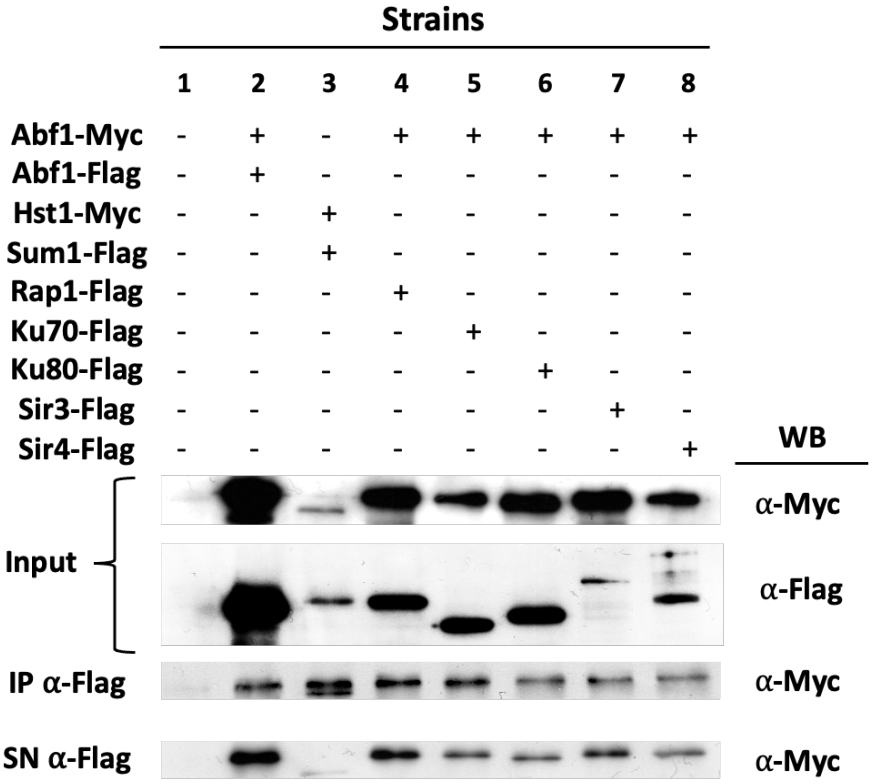

Figure 10 Abf1 interacts with silencing proteins. Total extracts were obtained from SP cells of the parental strain (BG14 untagged, lane 1), CGM3588 (Abf1-Myc/Abf1-Flag, lane 2), CGM1236 (Hst1-Myc/Sum1-Flag, lane 3), CGM4095 (Abf1-Myc/Rap1-Flag, lane 4), CGM4097 (Abf1-Myc/Ku70-Flag, lane 5), CGM4099 (Abf1-Myc/Ku80-Flag, lane 6), CGM4091 (Abf1-Myc/Sir3-Flag, lane 7), CGM4093 (Abf1-Myc/Sir4-Flag, lane 8). Extracts from these strains were analyzed by Western blot using antibody specific to the Flag and Myc epitopes for the detection of each corresponding tagged protein (Input). Extracts then were co-immunoprecipitated with antibodies specific to the Flag epitope and probed with antibodies specific to the Myc epitope (IP α-Flag, WB α-Myc). The recovered supernatant after immunoprecipitation with antibodies specific to Flag was analyzed using antibodies against Myc (SN α-Flag, WB α-Myc). IP, immunoprecipitation; WB, Western blot; SN, supernatant.

6.4. Sir4, yKu70 and yKu80 form foci at the nuclear periphery in *C. glabrata*

It has previously been shown that association of the telomeres to the nuclear periphery (NP) participates in TPE. The proteins involved in this mechanism in *S. cerevisiae* are Sir4, yKu70/80, and the C-terminal domain of Esc1 (Andrulis et al., 2002; Taddei et al., 2004). To evaluate if positioning of the telomeres to the nuclear envelop occurs also in *C. glabrata* we construct a battery of mutants where we tagged *Cg*Ku70::GFP, *Cg*Ku80::YFP, and *Cg*Sir4::GFP, as well as the nuclear envelop protein *Cg*Nup49 fused to mCherry to visualize the nuclear periphery by microscopy. We found that *Cg*Sir4*, Cg*Ku70*, and Cg*Ku80 colocalize with *Cg*Nup49 forming foci at the NP (Fig. 11). Our data suggest that *C. glabrata* might also anchor the telomeres to the nuclear envelop probably through *Cg*Sir4 and *Cg*Ku70/80.

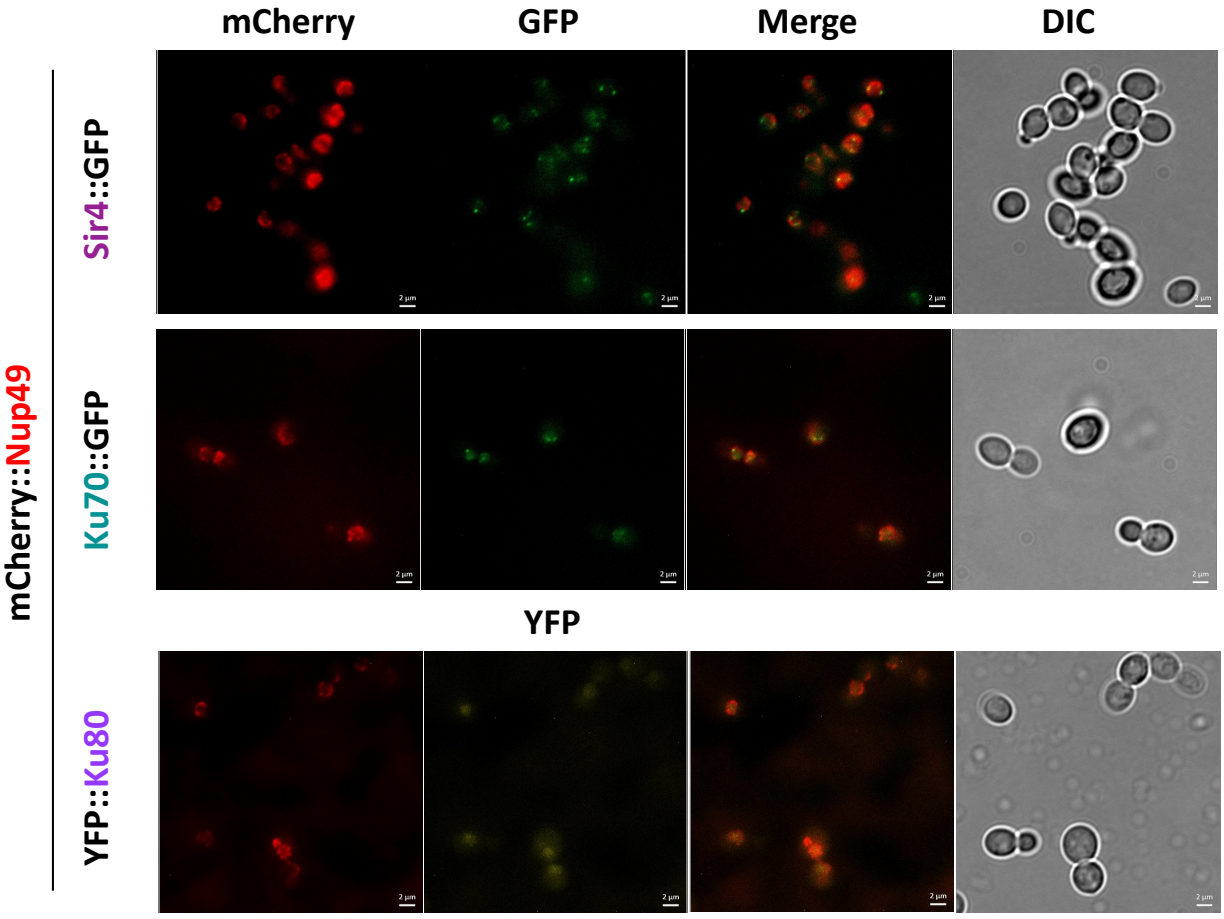

Figure 11 yKu and Sir4 are found in foci near the nuclear periphery in *C. glabrata*. Cells from LP grown in CAA were washed with 1 mL of Milli Q water, resuspended and the fluorescence visualized with the microscope Axio Imager.m2. From left to right, mCherry, GFP/YFP, merge (mCherry+GFP or mCherry+YFP), DIC (Differencial interference contrast). Scale corresponds to 2 µm.

6.5. *CgESC1* has no effect in silencing.

In *S. cerevisiae* Esc1 is key in the recruitment of the telomeres to the nuclear periphery and silencing of the adjacent genes found near the region (Andrulis et al., 2002). In *C. glabrata* there is an uncharacterized orthologue for *ESC1*, and we wanted to evaluate: a) if recruitment to the NP is involved in subtelomeric silencing in *C. glabrata* and b) whether the mechanism of telomere recruitment to the nuclear periphery depends on *CgESC1.* First, we deleted the *ESC1* from the genome and then we used the *URA3* reporter gene to measure the level of silencing using spot growth assays, we used different strain backgrounds where adhesin encoding genes are subject to subtelomeric silencing. We found that contrary to what is observed in *S. cerevisiae*, the absence of *ESC1* did not affect the silencing at different subtelomers (E-R, E-L, I-R, C-L) nor at the region 32 Kb away from telomere E-R (Fig. 12-14), with the insertion of Sil2126 at this position (Sil2126@-32 Kb).

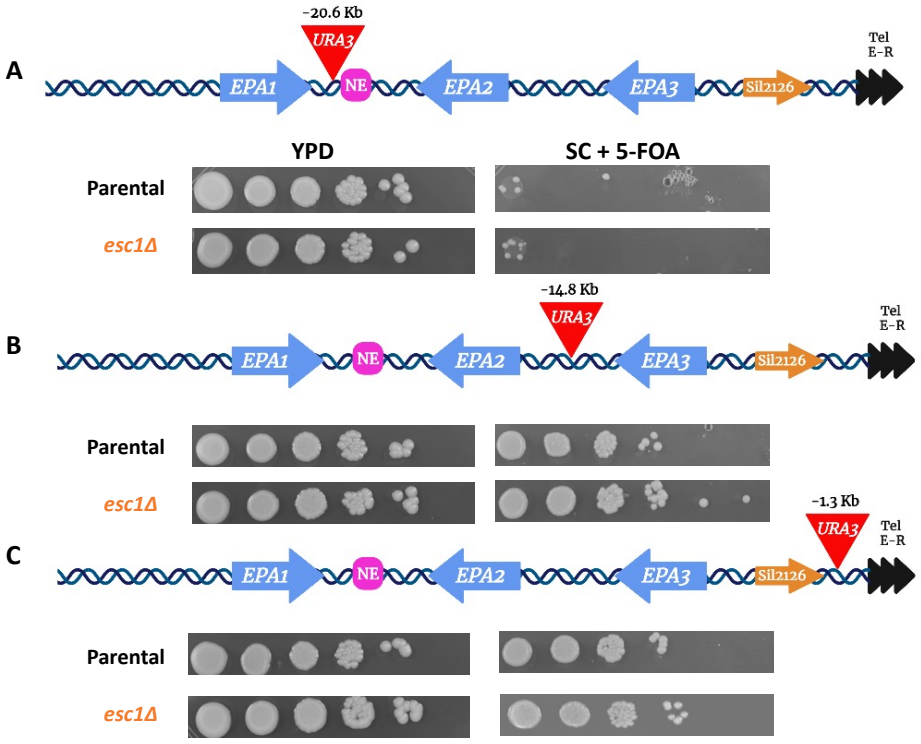

Figure 12 *esc1Δ* has no effect in subtelomeric silencing at the telomere E-R in *C. glabrata*. A; Schematic representation of the insertion of the *URA3* reporter between *EPA1* and NE. Silencing of *URA3* was measured in the parental strain (BG14) and *esc1Δ* background. B; Schematic representation of the insertion of *URA3* reporter between *EPA2* and *EPA3*. Silencing of *URA3* was measured in the parental strain (BG14) and *esc1Δ* background. C; Schematic representation

of the insertion of *URA3* reporter between protosilencer Sil2126 and the telomere. Silencing of *URA3* was measured in the parental strain (BG14) and *esc1Δ* background.

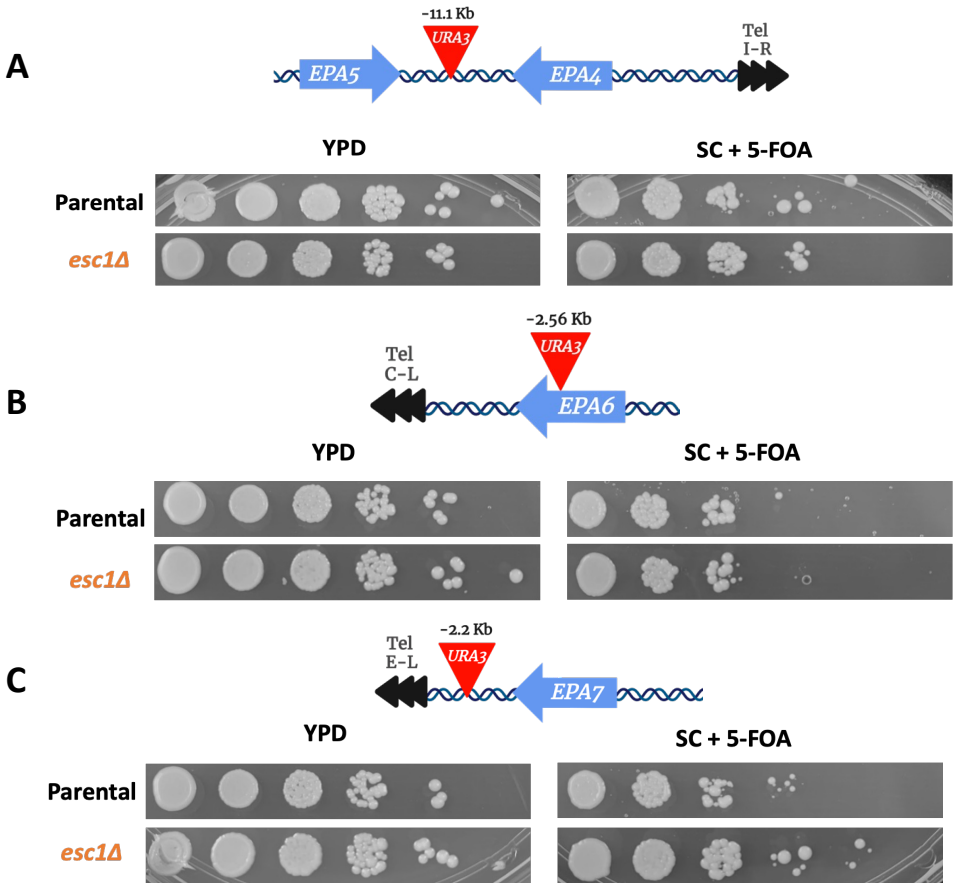

Figure 13 *esc1Δ* has no effect in silencing at other telomeres that harbor adhesin encoding genes. A; Schematic representation of the insertion of *URA3* reporter at the I-R telomere. Silencing of *URA3* was measured in the parental strain (BG14) and *esc1Δ* background. B; Schematic representation of the insertion of *URA3* reporter at the C-L telomere. Silencing of *URA3* was measured in the parental strain (BG14) and *esc1Δ* background. C; Schematic representation of the insertion of *URA3* reporter at the E-L telomere. Silencing of *URA3* was measured in the parental strain (BG14) and *esc1Δ* background.

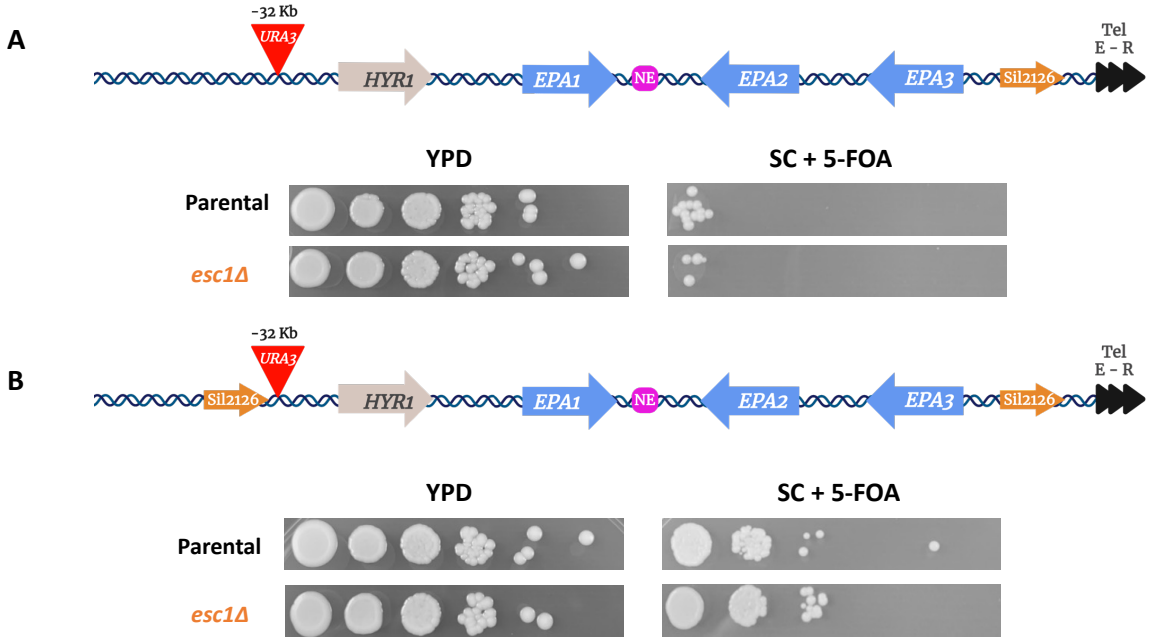

Figure 14 *esc1Δ* has no effect in subtelomeric silencing in a Sil2126@-32 Kb reporter system. A; Schematic representation of the *URA3* insertion at -32 Kb from the telomere E-R. Silencing of *URA3* was measured in the parental strain (BG14) and *esc1Δ* background. B; Schematic representation of the *URA3* insertion with Sil2126 at -32 Kb from the telomere E-R. Silencing of *URA3* was measured in the parental strain (BG14) and *esc1Δ* background.

Additionally, we evaluated if the absence of *HDF1* (encoding yKu70) or *HDF2* (encoding yKu80), in the *esc1*Δ background had an additional effect on silencing, results show that double mutants *hdf1*Δ/*esc1*Δ or *hdf2*Δ/*esc1*Δ do not show silencing the *URA3* reporter near the telomere where *EPA6* and *EPA7* are found (Fig. 15), that is the double mutants display the phenotype of the *hdf1*Δ or *hdf2*Δ single mutants.

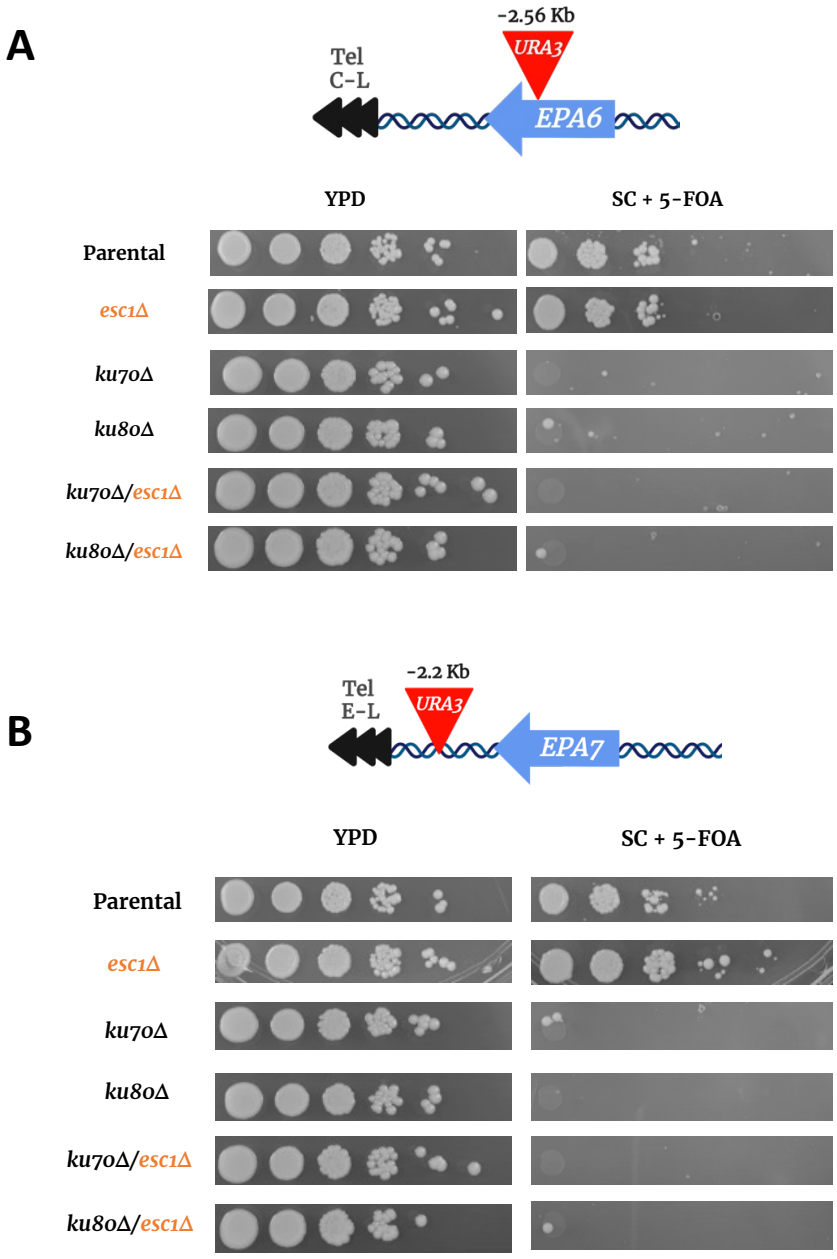

Figure 15 Absence of *ESC1* in *hdf1Δ* mutant background has no effect in silencing at telomeres C-L and E-L in *C. glabrata*. A; Schematic representation of the insertion of *URA3* reporter at the C-L telomere. Silencing of *URA3* was measured in the parental strain (BG14), mutants *esc1Δ, hdf1Δ, hdf2Δ,* and double mutants *esc1Δ/hdf1Δ* y *esc1Δ/hdf2Δ.* B; Schematic representation of the insertion of *URA3* reporter at the E-L telomere. Silencing of *URA3* was measured in the parental strain (BG14), mutants *esc1Δ, hdf1Δ, hdf2Δ,* and double mutants *esc1Δ/ku70Δ* y *esc1Δ/ku80Δ.*

6.6. *esc1*Δ mutant is temperature sensitive in *C. glabrata*

Previous data has shown that mutants in genes that encode proteins involved in telomere maintenance such as yKu complex are temperature sensitive, so we decided to evaluate if the absence of *ESC1* (associated to recruitment of the

telomeres to the NP), affects growth at high temperatures. We found that the *esc1*Δ strain was sensitive at 45ºC, in comparison to the parental strain, similar to the *hdf1*Δ strain (Fig. 16). This phenotype could suggest that *ESC1* might also impact telomere stability but does not play a role in silencing mediated by TPE in *C. glabrata*.

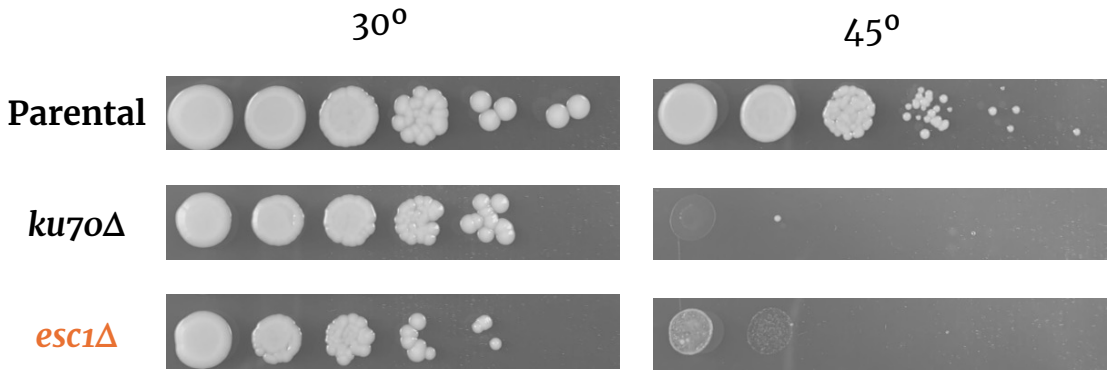

Figure 16 Esc1 is necessary for growth at high temperature in *C. glabrata*. Serial dilutions from stationary phase cells grown in rich media (YPD) were made ~ 3µL were spotted onto YPD plates and incubated at 30º and 45º, representative pictures of 48 h are shown. Parental strain (BG14), T^S *hdf1Δ* as control, and mutant strain *esc1Δ*.

7. Discussion

Chromatin structure and organization are key in many DNA metabolic processes. Hierarchical organization of the DNA is influenced by diverse factors, both *cis*-regulatory elements and *trans*-acting elements interactions that are dependent on external stimuli. In *C. glabrata* telomere loop conformations take place at telomere E-R where *EPA1, EPA2* and *EPA3* adhesin encoding genes form a cluster (López-Fuentes et al., 2018). Moreover, we found that this 3D conformation depends on protein-DNA and protein-protein interactions.

7.1. Abf1 and Rap1 bind at different positions throughout the telomere E-R and interact with each other.

In this work we found that Abf1 can interact with other silencing proteins, such as Rap1, Ku70, Ku80, Sir3, Sir4, and with itself (Fig. 10). We also found that Abf1 and Rap1 bind throughout different positions at the telomere E-R where we found several putative binding sites for both proteins. This is consistent with the 3C data and our model (López-Fuentes et al., 2018) where the *cis*-acting element, the protosilencer Sil2126, interacts with other *cis*-regulatory elements located at the intergenic regions in the telomere E-R. These *cis*-acting elements are localized at the intergenic region between *EPA2-EPA3* that is crucial for Sil2126 activity and contains many putative binding sites for Abf1 and Rap1 proteins. Interestingly, we found that Rap1 binds with higher frequency at *EPA2-EPA3* intergenic region and the tandem sequence repeats of the telomere E (Chapter 2) in comparison to sequences found further from the telomere. This suggests that heterochromatin establishment along the telomere E-R has different requirements as it spreads from the telomere to the adjacent subtelomeric region. Alternatively, the affinity of Rap1 and Abf1 to their respective binding sites along the region is different, so for example, Rap1 binds with higher affinity to the telomere than to other sites in the genome, therefore the recruitment of Rap1 might be influenced by its proximity to the telomere (Buchman et al., 1988; Conrad et al., 1990). On the contrary, Abf1 binds frequently to the regions distant from the telomere like intergenic region between *EPA1-EPA2* and the *EPA1* promoter.

7.2. Abf1 negatively regulates *EPA1* expression.

*Cg*Abf1 participates in subtelomeric silencing at telomere E-R and other telomeres that harbor adhesin encoding genes (Hernández-Hernández et al., 2021). Consistently, we found that Abf1 is recruited at several positions across the intergenic regions of the telomere E-R, including the *EPA1* promoter region. Moreover, we found that Abf1 negatively regulates the expression of *EPA1* and in an *abf1-43* truncated mutant that is defective for silencing, we observed a higher percentage of adherence to epithelial cells *in vitro*, suggesting that *EPA1* is derepressed in the *abf1-43* background (Chapter 2). Previous work has shown that *EPA1* expression is subject to multiple layers of negative regulation one of them independent from the silencing that comes from the telomere and mediated by the NE and yKu complex proteins (Gallegos-García et al., 2012). We suggest that Abf1 might be part of this mechanism that directly involves Abf1 binding to the promoter, the NE, and interaction with yKu proteins.

Another possibility is the one that involves the protosilencer Sil2126, which can recruit Abf1 and allows establishment of the subtelomeric silencing through the formation of a chromatin loop where *EPA1* regulatory regions are found within this loop hence blocking the recruitment of the transcription machinery. Although the interaction between Sil2126 and the promoter region of *EPA1* is not as frequent as other regions that are closer to this element, we suggest that this interaction is likely to change depending on the conditions to which the cells are subjected (López-Fuentes et al., 2018).

7.3. *ESC1* does not participate in subtelomeric silencing of *EPA* genes.

We found that *ESC1* has no clear effect in subtelomeric silencing at different telomeres in *C. glabrata* (Fig. 12-15). In *S. cerevisiae* anchor of the telomeres to the nuclear envelop is another mechanism involved in establishment of silencing, this mechanism requires the interaction of Esc1 with Sir4 and yKu complex proteins (Gotta et al., 1996; Taddei et al., 2004), however, this does not seem to be the case in *C. glabrata*.

We suggest that even tough *C. glabrata* possesses all the telomere tethering machinery, it might not result in silencing the subtelomeric genes, at least at the telomeres that we evaluated. Nevertheless, we have found that *Cg*Sir4, *Cg*Ku70, and *Cg*Ku80 localize near the nuclear periphery forming foci (Fig. 11), this is the first evidence that suggests that in *C. glabrata* telomeres might also cluster near the nuclear periphery, but this clustering does not result in silencing by itself. In *S. cerevisiae* telomere-anchoring pathways differ during the cell cycle, for instance, during G1, Sir4 interaction with yKu80 drives the telomeres to the nuclear vicinity, but during S-phase anchoring of the telomeres requires Esc1-Sir4 interaction (Taddei et al., 2004). Further work is aimed at establishing whether requirements for perinuclear anchoring changes during the cell cycle and whether this anchoring occurs in the absence of silencing at other telomeres.

8. Conclusion

Telomeres are crucial structures that help maintain DNA integrity, these regions contain complexes of proteins and sequences important to regulate its structure and stability throughout the life of the cell. In *C. glabrata* the right telomere of chromosome E, where *EPA1, EPA2*, and *EPA3* form a cluster, contains unique characteristics that make it an interesting model to study chromatin architecture and its implications in the regulation of genes involved in virulence like the adhesin-encoding genes.

Mechanisms like perinuclear anchoring of the telomeres and subtelomeric silencing depend on multiprotein complexes and *cis*-acting elements, that shape the telomere into different conformations in response to the environmental stimuli to which the cell is exposed.

In particular, the multifunctional protein *Cg*Abf1 participates in the subtelomeric silencing that negatively regulates the expression of *EPA1* and binds to different positions across the subtelomeric region, which suggests that *Cg*Abf1 not only influences the expression of *EPA1* but also contributes to establish silencing in regions distal from the telomere where it might recruit other silencing proteins like the ones from the SIR and yKu complexes, supporting the formation of 3D structures that maintain the silencing at the subtelomere.

8.1. Particular Conclusions

- *Cg*Abf1 is essential for cell viability in *C. glabrata.*
- *Cg*Abf1 negatively regulates *EPA1* expression.
- *Cg*Abf1 is implicated in DNA replication and correct cell cycle progression.
- *Cg*Abf1 binds to its own promoter region.
- *Cg*Abf1 and *Cg*Rap1 are distributed along different regions through the telomere E-R.
- Silencing proteins *Cg*Abf1, *Cg*Rap1, *Cg*Ku70/80, *Cg*Sir3 and *Cg*Sir4 can form a complex.
- *Cg*Sir4 and *Cg*Ku70/80 can be found at the nuclear periphery.

9. Perspectives

- Characterize protein complex of Abf1 with the rest of the silencing proteins, under stress conditions like oxidative stress and biofilm formation by Mass Spectrophotometry.
- Characterize the chromatin conformation in the absence of Abf1 or in the absence of silencing using Chromatin Conformation Capture Assay (3C-assay).
- Determine the role of Esc1 in telomere tethering to the nuclear envelope, and its interaction with other proteins like Sir4 and yKu complex to anchor telomeres to the nuclear periphery using confocal microscopy.
- Determine if Esc1's role in telomere anchoring has an effect in silencing establishment, and/or if it does not lead to spreading of silencing to the adjacent region of the telomere.
- Determine if there are other proteins that mediate telomere tethering at the nuclear periphery.

10. References

Abraham, J., Nasmyth, K.A., Strathern Amar, J.N., Klar, J.S., Hicks, J.B., 1984. Regulation of Mating-type Information in Yeast. J. Mol. BioE 176, 307–331.

Ai, W., Bertram, P.G., Tsang, C.K., Chan, T.F., Zheng, X.F.S., 2002. Regulation of subtelomeric silencing during stress response. Mol Cell 10, 1295–1305. https://doi.org/10.1016/S1097-2765(02)00695-0

Andrulis, E.D., Neiman, A.M., Zappulla, D.C., Sternglanz, R., 1998. Perinuclear localization of chromatin facilitates transcriptional silencing. Nature 394, 592–595. https://doi.org/10.1038/29100

Andrulis, E.D., Zappulla, D.C., Ansari, A., Perrod, S., Laiosa, C. V., Gartenberg, M.R., Sternglanz, R., 2002. Esc1, a Nuclear Periphery Protein Required for Sir4-Based Plasmid Anchoring and Partitioning. Mol Cell Biol 22, 8292–8301. https://doi.org/10.1128/mcb.22.23.8292-8301.2002

Beisel, C., Paro, R., 2011. Silencing chromatin: comparing modes and mechanisms. Nat Rev Genet 12, 123–135. https://doi.org/10.1038/nrg2932

Bi, X., Braunstein, M., Shei, G.J., Broach, J.R., 1999. The yeast HML I silencer defines a heterochromatin domain boundary by directional establishment of silencing. Proc Natl Acad Sci U S A 96, 11934–9. https://doi.org/10.1073/pnas.96.21.11934

Bonetti, D., Clerici, M., Anbalagan, S., Martina, M., Lucchini, G., Longhese, M.P., 2010. Shelterin-like proteins and Yku inhibit nucleolytic processing of Saccharomyces cerevisiae telomeres. PLoS Genet 6, 1. https://doi.org/10.1371/journal.pgen.1000966

Boscheron, C., Maillet, L., Marcand1, S., Tsai-Pflugfelder2, M., Gasser2, S.M., Gilson3, E., 1996. Cooperation at a distance between silencers and proto-silencers at the yeast HML locus, The EMBO Journal.

Boulton, S.J., Jackson, S.P., 1998. Components of the Ku-dependent non-homologous end-joining pathway are involved in telomeric length maintenance and telomeric silencing, The EMBO Journal.

Boulton, S.J., Jackson, S.P., 1996. Identification of a Saccharomyces cerevisiae Ku80 homologue: roles in DNA double strand break rejoining and in telomeric maintenance, Nucleic Acids Research.

Buchman, A.R., Kimmerly, W.J., Rine, J., Kornberg, R.D., 1988. Two DNA-Binding Factors Recognize Specific Sequences at Silencers, Upstream Activating Sequences, Autonomously Replicating Sequences, and Telomeres in Saccharomyces cerevisiae 8, 210–225.

Buck, S.W., Shore, D., 1995. Action of a RAP1 carboxy-terminal silencing domain reveals an underlying competition between HMR and telomeres m yeas.

Calvin, N.M., Hanawalt, P.C., 1988. High-efficiency transformation of bacterial cells by electroporation. J Bacteriol 170, 2796–2801. https://doi.org/10.1128/jb.170.6.2796-2801.1988

Castaño, I., Kaur, R., Pan, S., Cregg, R., De Las Peñas, A., Guo, N., Biery, M.C., Craig, N.L., Cormack, B.P., 2003. Tn7-based genome-wide random insertional mutagenesis of Candida glabrata. Genome Res 13, 905–915. https://doi.org/10.1101/gr.848203

Castaño, I., Pan, S.J., Zupancic, M., Hennequin, C., Dujon, B., Cormack, B.P., 2005. Telomere length control and transcriptional regulation of subtelomeric adhesins in Candida glabrata. Mol Microbiol 55, 1246–1258. https://doi.org/10.1111/j.1365-2958.2004.04465.x

Castaño, I., Kaur, R., Pan, S., Cregg, R., De Las Peñas, A., Guo, N., Biery, M.C., Craig, N.L., Cormack, B.P., 2003. Tn7-based genome-wide random insertional mutagenesis of Candida glabrata. Genome Res 13, 905–915. https://doi.org/10.1101/gr.848203

Cockell, M., Palladino, F., Laroche, T., Kyrion, G., Liu, C., Lustig, A.J., Gasser, S.M., 1995. The carboxy termini of Sir4 and RAP1 affect Sir3 localization: Evidence for a multicomponent complex required for yeast telomeric silencing. Journal of Cell Biology 129, 909–924. https://doi.org/10.1083/jcb.129.4.909

Conrad, M.N., Wright', J.H., Wolf, A.J., Zakian, V.A., 1990. RAP1 Protein Interacts with Yeast Telomeres In Vivo: Overproduction Alters Telomere Structure and Decreases Chromosome Stability, Cell.

Cormack, B.P., Ghori, N., Falkow, S., 1999a. An adhesin of the yeast pathogen Candida glabrata mediating adherence to human epithelial cells. Science 285, 578–582. https://doi.org/10.1126/science.285.5427.578

Cosgrove, A.J., Nieduszynski, C.A., Donaldson, A.D., 2002. Ku complex controls the replication time of DNA in telomere regions. Genes Dev 16, 2485–2490. https://doi.org/10.1101/gad.231602

De Boer, M., Nielsen, P.S., Bebelman, J.-P., Van Heerikhuizen, H., Andersen, H.A., Planta, R.J., 2000. Stp1p, Stp2p and Abf1p are involved in regulation of expression of the amino acid transporter gene BAP3 of Saccharomyces cerevisiae, Nucleic Acids Research.

De Groot, P.W.J., Kraneveld, E.A., Qing, Y.Y., Dekker, H.L., Groß, U., Crielaard, W., De Koster, C.G., Bader, O., Klis, F.M., Weig, M., 2008. The cell wall of the human pathogen Candida glabrata: Differential incorporation of novel adhesin-like wall proteins. Eukaryot Cell 7, 1951–1964. https://doi.org/10.1128/EC.00284-08

De Las Peñas, A., Pan, S.J., Castaño, I., Alder, J., Cregg, R., Cormack, B.P., 2003a. Virulence-related surface glycoproteins in the yeast pathogen Candida glabrata are encoded in subtelomeric clusters and subject to RAP1- and SIR-dependent transcriptional silencing. Genes Dev 17, 2245–2258. https://doi.org/10.1101/gad.1121003

Della Seta, F., Ciafre, S., Marck, C., Santoro, B., Presutti, C., Sentenac, A., Bozzoni, I., 1990. The ABF1 Factor Is the Transcriptional Activator of the L2 Ribosomal Protein Genes in Saccharomyces cerevisiae, MOLECULAR AND CELLULAR BIOLOGY.

Diffley, J.F.X., Stillman, B., 1988. Purification of a yeast protein that binds to origins of DNA replication and a transcriptional silencer (autonomously replicating sequence-binding factor/Saccharomyces cerevisiae/mating type regulation/site-specific DNA binding), Proc. Nati. Acad. Sci. USA.

Domergue, R., Castaño, I., De Las Peñas, A., Zupancic, M., Lockatell, V., Hebel, J.R., Johnson, D., Cormack, B.P., 2005. Nicotinic acid limitation regulates silencing of Candida adhesins during UTI. Science (1979) 308, 866–870. https://doi.org/10.1126/science.1108640

Elledge, S.J., Davis, R.W., 1989. Identification of the DNA Damage-Responsive Element of RNR2 and Evidence that Four Distinct Cellular Factors Bind It, MOLECULAR AND CELLULAR BIOLOGY.

Fabre, E., Muller, H., Therizols, P., Lafontaine, I., Dujon, B., Fairhead, C., 2005. Comparative genomics in hemiascomycete yeasts: Evolution of sex, silencing, and subtelomeres. Mol Biol Evol 22, 856–873. https://doi.org/10.1093/molbev/msi070

Feng, L., Wang, B., Jong, A., 1998. Saccharomyces cerevisiae Cdc6 stimulates Abf1 DNA binding activity. Journal of Biological Chemistry 273, 1298–1302. https://doi.org/10.1074/jbc.273.3.1298

Fermi, B., Bosio, M.C., Dieci, G., Bioscienze, D., Area, P., 2016. Promoter architecture and transcriptional regulation of Abf1-dependent ribosomal protein genes in Saccharomyces cerevisiae 1–14. https://doi.org/10.1093/nar/gkw194

Fourel, G., Revardel, E., Koering, C.E., Gilson, ??ric, 1999. Cohabitation of insulators and silencing elements in yeast subtelomeric regions. EMBO Journal 18, 2522–2537. https://doi.org/10.1093/emboj/18.9.2522

Gabaldón, T., Martin, T., Marcet-Houben, M., Durrens, P., Bolotin-Fukuhara, M., Lespinet, O., Arnaise, S., Boisnard, S., Aguileta, G., Atanasova, R., Bouchier, C., Couloux, A., Creno, S., Almeida Cruz, J., Devillers, H., Enache-Angoulvant, A., Guitard, J., Jaouen, L., Ma, L., Marck, C., Neuvéglise, C., Pelletier, E., Pinard, A., Poulain, J., Recoquillay, J., Westhof, E., Wincker, P., Dujon, B., Hennequin, C., Fairhead, C., 2013. Comparative genomics of emerging pathogens in the Candida glabrata clade. BMC Genomics 14. https://doi.org/10.1186/1471-2164-14-623

Gallegos-García, V., Pan, S.J., Juárez-Cepeda, J., Ramírez-Zavaleta, C.Y., Martin-del-Campo, M.B., Martínez-Jiménez, V., Castaño, I., Cormack, B., Peñas, A. de Las, 2012a. A novel downstream regulatory element cooperates with the silencing machinery to repress EPA1 expression in candida glabrata. Genetics 190, 1285–1297. https://doi.org/10.1534/genetics.111.138099

Gilson, E., Roberge, M., Giraldo, R., Rhodes, D., Gasser, S., 1993. Distortion of the DNA Double Helix by RAP1 at Silencers and Multiple Telomeric Binding Sites. Journal of Molecular Biology 231, 293–310.

Gotta, M., Laroche, T., Formenton, A., Maillet, L., Scherthan, H., Gasser, S.M., 1996. The clustering of telomeres and colocalization with Rap1, Sir3, and Sir4 proteins in wild-type Saccharomyces cerevisiae. Journal of Cell Biology 134, 1349–1363. https://doi.org/10.1083/jcb.134.6.1349

Gottschling, D.E., Aparicio, O.M., Billington, B.L., Zakiant, V.A., 1990. Position Effect at S. cerevisiae Telomeres: Reversible Repression of Pol II Transcription, Cell.

Gravel, S., Wellinger, R.J., 2002. Maintenance of Double-Stranded Telomeric Repeats as the Critical Determinant for Cell Viability in Yeast Cells Lacking Ku. Mol Cell Biol 22, 2182–2193. https://doi.org/10.1128/mcb.22.7.2182-2193.2002

Grunstein, M., Gasser, S.M., 2013. Epigenetics in Saccharomyces cerevisiae. Cold Spring Harb Perspect Biol 5, 1–28. https://doi.org/10.1101/cshperspect.a017491

Gutiérrez-Escobedo, G., Hernández-Carreón, O., Morales-Rojano, B., Revuelta-Rodríguez, B., Vázquez-Franco, N., Castaño, I., De Las Peñas, A., 2020a. Candida glabrata peroxiredoxins, Tsa1 and Tsa2, and sulfiredoxin, Srx1, protect against oxidative damage and are necessary for virulence. Fungal Genetics and Biology 135, 103287. https://doi.org/10.1016/j.fgb.2019.103287

Hardy, C.F.J., Sussel, L., Shore^, D., 1992. A RAP 1-interacting protein involved in transcriptional silencing and telomere length regulation.

Hediger, F., Gasser, S.M., 2002. Nuclear organization and silencing: Putting things in their place. Nat Cell Biol 4, 53–55. https://doi.org/10.1038/ncb0302-e53

Helmstetter, N., Chybowska, A.D., Delaney, C., Da Silva Dantas, A., Gifford, H., Wacker, T., Munro, C., Warris, A., Jones, B., Cuomo, C.A., Wilson, D., Ramage, G., Farrer, R.A., 2022. Population genetics and microevolution of clinical Candida glabrata reveals recombinant sequence types and hyper-variation within mitochondrial

genomes, virulence genes, and drug targets. Genetics 221. https://doi.org/10.1093/genetics/iyac031
Hernández-Hernández, G., Vera-Salazar, L.A., Castanedo, L., López-Fuentes, E., Gutiérrez-Escobedo, G., De Las Peñas, A., Castaño, I., 2021a. Abf1 is an essential protein that participates in cell cycle progression and subtelomeric silencing in candida glabrata. Journal of Fungi 7. https://doi.org/10.3390/jof7121005
Juárez-Cepeda, J., Orta-Zavalza, E., Cañas-Villamar, I., Arreola-Gómez, J., Pérez-Cornejo, G.P., Hernández-Carballo, C.Y., Gutiérrez-Escobedo, G., Castaño, I., De Las Peñas, A., 2015a. The EPA2 adhesin encoding gene is responsive to oxidative stress in the opportunistic fungal pathogen Candida glabrata. Curr Genet 61, 529–544. https://doi.org/10.1007/s00294-015-0473-2
Juárez-Reyes, A., Ramírez-Zavaleta, C.Y., Medina-Sánchez, L., de Las Peñas, A., Castaño, I., 2012a. A protosilencer of subtelomeric gene expression in Candida glabrata with unique properties. Genetics 190, 101–111. https://doi.org/10.1534/genetics.111.135251
Kirkland, J.G., Peterson, M.R., Still, C.D., Brueggeman, L., Dhillon, N., Kamakaka, R.T., 2015. Heterochromatin formation via recruitment of DNA repair proteins. Mol Biol Cell 26, 1395–1410. https://doi.org/10.1091/mbc.E14-09-1413
Kovari, L.Z., Cooper, T.G., 1991. Participation of ABF-1 Protein in Expression of the Saccharomyces cerevisiae CAR] Gene, JOURNAL OF BACTERIOLOGY.
Kraneveld, E.A., de Soet, J.J., Deng, D.M., Dekker, H.L., de Koster, C.G., Klis, F.M., Crielaard, W., de Groot, P.W.J., 2011a. Identification and Differential Gene Expression of Adhesin-Like Wall Proteins in Candida glabrata Biofilms. Mycopathologia 172, 415–427. https://doi.org/10.1007/s11046-011-9446-2
Mycopathologia 172, 415–427. https://doi.org/10.1007/s11046-011-9446-2
Kueng, S., Oppikofer, M., Gasser, S.M., 2013. SIR Proteins and the Assembly of Silent Chromatin in Budding Yeast. Annu Rev Genet 47, 275–306. https://doi.org/10.1146/annurev-genet-021313-173730
Lebrun, É., Revardel, E., Boscheron, C., Li, R., Gilson, E., Fourel, G., 2001. Protosilencers in Saccharomyces cerevisiae subtelomeric regions. Genetics 158, 167–176.
Levy, D.L., Blackburn, E.H., 2004. Counting of Rif1p and Rif2p on Saccharomyces cerevisiae Telomeres Regulates Telomere Length. Mol Cell Biol 24, 10857–10867. https://doi.org/10.1128/mcb.24.24.10857-10867.2004
Lipford, J.R., Bell, S.P., 2001. Nucleosomes Positioned by ORC Facilitate the Initiation of DNA Replication text can significantly alter origin function. For example, many potential origins of replication function well in the context of a plasmid, but poorly or not at all in their, Molecular Cell.
López-Fuentes, E., Hernández-Hernández, G., Castanedo, L., Gutiérrez-Escobedo, G., Oktaba, K., De las Peñas, A., Castaño, I., 2018a. Chromatin loop formation induced by a subtelomeric protosilencer represses EPA genes in Candida glabrata. Genetics 210, 113–128. https://doi.org/10.1534/genetics.118.301202
Luo, K., Vega-Palas, M.A., Grunstein, M., 2002. Rap1-Sir4 binding independent of other Sir, yKu, or histone interactions initiates the assembly of telomeric heterochromatin in yeast. Genes Dev 16, 1528–1539. https://doi.org/10.1101/gad.988802
Marcand, S., Gilson, E., Shore, D., 1997. A Protein-Counting Mechanism for Telomere Length Regulation in Yeast. Science (1979) 275, 986–990.
Martínez-Jiménez, V., Ramírez-Zavaleta, C.Y., Orta-Zavalza, E., Díaz de León, G., Gutiérrez-Escobedo, G., Ponce de León, A., Sifuentes-Osornio, J., Bobadilla del Valle,

M., De Las Peñas, A., Castaño, I., 2013. Sir3 Polymorphisms in Candida glabrata Clinical Isolates. Mycopathologia 175, 207–219. https://doi.org/10.1007/s11046-013-9627-2
Miyake, T., Loch, C.M., Li, R., 2002. Identification of a Multifunctional Domain in Autonomously Replicating Sequence-Binding Factor 1 Required for Transcriptional Activation, DNA Replication, and Gene Silencing. Mol Cell Biol 22, 505–516. https://doi.org/10.1128/MCB.22.2.505-516.2002
Miyake, T., Reese, J., Loch, C.M., Auble, D.T., Li, R., 2004. Genome-wide Analysis of ARS (Autonomously Replicating Sequence) Binding Factor 1 (Abf1p) -mediated Transcriptional Regulation in 279, 34865–34872. https://doi.org/10.1074/jbc.M405156200
Moretti, P., Shore, D., 2001. Multiple interactions in Sir protein recruitment by Rap1p at silencers and telomeres in yeast. Mol Cell Biol 21, 8082–94. https://doi.org/10.1128/MCB.21.23.8082-8094.2001
Orta-Zavalza, E., Guerrero-Serrano, G., Gutiérrez-Escobedo, G., Cañas-Villamar, I., Juárez-Cepeda, J., Castaño, I., De Las Peñas, A., 2013. Local silencing controls the oxidative stress response and the multidrug resistance in Candida glabrata. Mol Microbiol 88, 1135–1148. https://doi.org/10.1111/mmi.12247
Ozsarac, N., Straffon, M.J., Dalton, H.E., Dawes, I.W., 1997. Regulation of Gene Expression during Meiosis in Saccharomyces cerevisiae: SPR3 Is Controlled by both ABFI and a New Sporulation Control Element, MOLECULAR AND CELLULAR BIOLOGY.
Palladino, F., Laroche, T., Gilson, E., 1993. SIR3 and SIR4 Proteins Are Required for the Positioning and Integrity of Yeast Telomeres 75, 543–555.
Pfeiffer, V., Lingner, J., 2013. Replication of telomeres and the regulation of telomerase. Cold Spring Harb Perspect Biol 5. https://doi.org/10.1101/cshperspect.a010405
Planta, R.J., 1997. Regulation of ribosome synthesis in yeast. Yeast 13, 1505–1518. https://doi.org/10.1002/(SICI)1097-0061(199712)13:16<1505::AID-YEA229>3.0.CO;2-I
Ramírez-Zavaleta, C.Y., Salas-Delgado, G.E., de Las Peñas, A., Castaño, I., 2010. Subtelomeric silencing of the MTL3 locus of Candida glabrata requires yKu70, yKu80, and Rif1 proteins. Eukaryot Cell 9, 1602–1611. https://doi.org/10.1128/EC.00129-10
Reed, S.H., Akiyama, M., Stillman, B., Friedberg, E.C., 1999. Yeast autonomously replicating sequence binding factor is involved in nucleotide excision repair 4, 3052–3058.
Rhode, P.R., Sweder, K.S., Oegema, K.F., Campbell, J.L., 1989a. The gene encoding ARS-binding factor I is essential for the viability of yeast.
Rie Gailus-Durner, V., Xie, J., Chintamaneni, C., Vershon, A.K., 1996. Participation of the Yeast Activator Abf1 in Meiosis-Specific Expression of the HOP1 Gene, MOLECULAR AND CELLULAR BIOLOGY.
Rine, J., Herskowitz, I., 1987. Four Genes Responsible for a Position Effect on Expression From HML and HMR in Saccharomyces cerevisiae. Genetics 116, 9-22.
Rine, J., Strathern, J.N., Hicks, J.B., Herskowitz, I., 1979. A Supressor of Mating-Type locus mutations in Saccharomyces cerevisisae. Genetics 93, 877–901.
Roetzer, A., Gregori, C., Jennings, A.M., Quintin, J., Ferrandon, D., Butler, G., Kuchler, K., Ammerer, G., Schüller, C., 2008. Candida glabrata environmental stress response

involves Saccharomyces cerevisiae Msn2/4 orthologous transcription factors. Mol Microbiol 69, 603–620. https://doi.org/10.1111/j.1365-2958.2008.06301.x
Rosas-Hernández, L.L., Juárez-Reyes, A., Arroyo-Helguera, O.E., De Las Peñas, A., Pan, S.J., Cormack, B.P., Castaño, I., 2008. yKu70/yKu80 and Rif1 regulate silencing differentially at telomeres in Candida glabrata. Eukaryot Cell 7, 2168–2178. https://doi.org/10.1128/EC.00228-08
Rusché, L.N., Kirchmaier, A.L., Rine, J., 2002. Ordered nucleation and spreading of silenced chromatin in Saccharomyces cerevisiae. Mol Biol Cell 13, 2207–2222. https://doi.org/10.1091/mbc.E02-03-0175
Schmitt, M.E., Brown, T.A., Trumpower, B.L., 1990. A rapid and simple method for preparation of RNA from Saccharomyces cerevisiae. Nucleic Acids Res 18, 3091–3092. https://doi.org/10.1093/nar/18.10.3091
Sexton, T., Yaffe, E., Kenigsberg, E., Bantignies, F., Leblanc, B., Hoichman, M., Parrinello, H., Tanay, A., Cavalli, G., 2012. Three-dimensional folding and functional organization principles of the Drosophila genome. Cell 148, 458–472. https://doi.org/10.1016/j.cell.2012.01.010
Shore, D., Nasmyth, K., 1987. Purification and Cloning of a DNA Binding Protein from Yeast That Binds to Both Silencer and Activator Elements, Cell.
Strahl-Bolsinger, S., Hecht, A., Luo, K., Grunstein, M., 1997. SIR2 and SIR4 interactions differ in core and extended telomeric heterochromatin in yeast. Genes Dev 11, 83–93. https://doi.org/10.1101/gad.11.1.83
Taddei, A., Hediger, F., Neumann, F.R., Bauer, C., Gasser, S.M., 2004. Separation of silencing from perinuclear anchoring functions in yeast Ku80, Sir4 and Esc1 proteins. EMBO J 23, 1301–12. https://doi.org/10.1038/sj.emboj.7600144
Teixeira, M.T., Gilson, E., 2005. Telomere maintenance, function and evolution: The yeast paradigm. Chromosome Research 13, 535–548. https://doi.org/10.1007/s10577-005-0999-0
Trawick, J.D., Kraut, N., Simon, F.R., Poyton, R. 0, 1992. Regulation of Yeast COX6 by the General Transcription Factor ABF1 and Separate HAP2-and Heme-Responsive Elements, MOLECULAR AND CELLULAR BIOLOGY.
Vignais, M.L., Woudt, L.P., Wassenaar, G.M., Mager, W.H., Sentenac, A., Planta, R.J., 1987. Specific binding of TUF factor to upstream activation sites of yeast ribosomal protein genes. EMBO J 6, 1451–1457. https://doi.org/10.1002/j.1460-2075.1987.tb02386.x
Wittkopp, P.J., Kalay, G., 2012. Cis-regulatory elements: Molecular mechanisms and evolutionary processes underlying divergence. Nat Rev Genet. https://doi.org/10.1038/nrg3095
Wotton, D., Shore, D., 1997. A novel Raplp-interacting factor, Rif2p, cooperates with Riflp to regulate telomere length in Saccharomyces cerevisiae.
Xu, Z., Green, B., Benoit, N., Schatz, M., Wheelan, S., Cormack, B., 2020. De novo genome assembly of Candida glabrata reveals cell wall protein complement and structure of dispersed tandem repeat arrays. Mol Microbiol 113, 1209–1224. https://doi.org/10.1111/mmi.14488
Xu, Z., Green, B., Benoit, N., Sobel, J.D., Schatz, M.C., Wheelan, S., Cormack, B.P., 2021. Cell wall protein variation, break-induced replication, and subtelomere dynamics in Candida glabrata. Mol Microbiol 116, 260–276. https://doi.org/10.1111/mmi.14707
Yáñez-Carrillo, P., Orta-Zavalza, E., Gutiérrez-Escobedo, G., Patrón-Soberano, A., De Las Peñas, A., Castaño, I., 2015. Expression vectors for C-terminal fusions with

fluorescent proteins and epitope tags in Candida glabrata. Fungal Genetics and Biology 80, 43–52. https://doi.org/10.1016/j.fgb.2015.04.020
Yarragudi, A., Miyake, T., Li, R., Morse, R.H., 2004. Comparison of ABF1 and RAP1 in Chromatin Opening and Transactivator Potentiation in the Budding Yeast Saccharomyces cerevisiae Comparison of ABF1 and RAP1 in Chromatin Opening and Transactivator Potentiation in the Budding Yeast Saccharomyces cerevisiae. Mol Cell Biol 24, 9152–9164. https://doi.org/10.1128/MCB.24.20.9152
Zaman, Z., Heid, C., Ptashne, M., 2002. Telomere looping permits repression “at a distance” in yeast. Current Biology 12, 930–933. https://doi.org/10.1016/S0960-9822(02)00865-5

11. Supplementary information

Other publications where I have participated:

Research article

- Hernández-Carreón O, Hernández-Howell C, Hernández-Hernández G, Herrera-Basurto MS, González-Gómez BE, Gutiérrez-Escobedo G, García-Calderón NI, Barrón-Pastor D, De Las Peñas A, Castaño I. Highly specific and rapid molecular detection of Candida glabrata in clinical samples. Braz J Microbiol. 2021 Dec;52(4):1733-1744. doi: 10.1007/s42770-021-00584-2. Epub 2021 Jul 31. PMID: 34331680; PMCID: PMC8578511.

Brazilian Journal of Microbiology (2021) 52:1733–1744
https://doi.org/10.1007/s42770-021-00584-2

BACTERIAL, FUNGAL AND VIRUS MOLECULAR BIOLOGY - RESEARCH PAPER

Highly specific and rapid molecular detection of *Candida glabrata* in clinical samples

Oscar Hernández-Carreón[1] · Cesia Hernández-Howell[1] · Grecia Hernández-Hernández[1] · M. Selene Herrera-Basurto[1] · Blanca E. González-Gómez[1] · Guadalupe Gutiérrez-Escobedo[1] · Norma I. García-Calderón[1] · Daniel Barrón-Pastor[1] · Alejandro De Las Peñas[1] · Irene Castaño[1]

Received: 23 September 2020 / Accepted: 18 July 2021 / Published online: 31 July 2021
© Sociedade Brasileira de Microbiologia 2021

Abstract
The most common nosocomial fungal infections are caused by several species of *Candida*, of which *Candida glabrata* is the second most frequently isolated species from bloodstream infections. *C. glabrata* displays relatively high minimal inhibitory concentration values (MIC) to the antifungal fluconazole and is associated with high mortality rates. To decrease mortality rates, the appropriate treatment must be administered promptly. *C. glabrata* contains in its genome several non-identical copies of species-specific sequences. We designed three pairs of *C. glabrata*-specific primers for endpoint PCR amplification that align to these species-specific sequences and amplify the different copies in the genome. Using these primers, we developed a fast, sensitive, inexpensive, and highly specific PCR-based method to positively detect *C. glabrata* DNA in a concentration-dependent manner from mixes of purified genomic DNA of several *Candida* species, as well as from hemocultures and urine clinical samples. This tool can be used for positive identification of *C. glabrata* in the clinic.

Keywords Molecular detection · *Candida glabrata* · Species-specific sequences · PCR amplification · Responsible Editor: Sandro Rogerio de Almeida

Book Chapter: *Candida* Species

- López-Fuentes, E., Hernández-Hernández, G., De Las Peñas, A., Castaño, I. (2022). Subtelomeric Chromatin Structure by Chromosome Conformation Capture (3C)-qPCR Methodology in *Candida glabrata*. In: Calderone, R. (eds) Candida Species. Methods in Molecular Biology, vol 2542. Humana, New York, NY. https://doi.org/10.1007/978-1-0716-2549-1_5

Chapter 5

Subtelomeric Chromatin Structure by Chromosome Conformation Capture (3C)-qPCR Methodology in *Candida glabrata*

Eunice López-Fuentes, Grecia Hernández-Hernández, Alejandro De Las Peñas, and Irene Castaño

Abstract

Chromatin architecture has an enormous impact on gene regulation, DNA replication, repair, and packaging. Chromatin is organized in a complex hierarchical manner in which distant fragments of DNA can interact with each other through DNA loops. DNA loops can interact between themselves to form topologically associated domains (TADs) that are further organized into functional compartments. In the last two decades, Chromatin Conformation Capture (3C technology) and its high-throughput derivatives allowed detailed analysis of the chromatin architecture. The 3C method is based on ligation of distant fragments brought together by DNA looping. The method analyzes a particular genomic region of interest and quantifies the interactions between a defined fragment with all the surrounding fragments of the region. It consists of four steps: (1) The long-distance interacting chromatin fragments are fixed with formaldehyde in whole cells which are then lysed; (2) the fixed chromatin is digested with a carefully chosen restriction enzymes to separate intervening DNA fragments; (3) the fragments brought into proximity by DNA looping are ligated in conditions favoring intramolecular ligation; and (4) the interactions are quantified by quantitative PCR using the TaqMan technology and unidirectional primers. Herein, we describe the use of this methodology to analyze the chromatin conformation at a subtelomeric *locus* containing three genes encoding adhesins and several *cis*-regulatory elements, in the pathogenic yeast *Candida glabrata*.

Key words 3C-qPCR, Chromatin interactions, Chromatin loops, *Candida glabrata*, *Cis*-acting elements, Nuclear architecture, TADs

12. Supplementary tables

Table S 1 Strains

E. coli	**Use**	**Genotype**	**Reference**
DH10B	Electrocompetent cells	F$^-$ *mcrA*Δ(*mrr-hsdRMS-mcrBC*) *80dlacZ*Δ*M15* Δ*lacX74 deoR recA1 endA1 araD139* Δ*(ara,leu)7697 galU galK* $^-$ *rpsL nupG*	(Calvin and Hanawalt, 1988)
C. glabrata	**Parental**	**Genotype**	**Reference**
BG14	BG2	*ura3*Δ::Tn*903* G418^R	(Cormack et al., 1999)
***URA3* insertions**			
CGM118	BG14	*ura3*Δ::Tn903 G418^R *EPA6*::Tn7 986 bp upstream stop codon (pSP121 *EcoR*I)	(Castaño et al., 2005)
CGM121	BG14	*ura3*Δ*::*Tn903 G418^R *EPA7* 3'UTR::Tn7 268 bp downstream stop codon (pIC44/*Kpn*I/*Bcg*I)	(Castaño et al., 2005)
CGM159	BG14	*ura3*Δ*::*Tn903 G418^R Tn7 at the intergenic region between *EPA5* and *EPA4* (pAP534/*Bcg*I)	(De Las Peñas et al., 2003)
CGM160	BG14	*ura3*Δ*::*Tn903 G418^R Tn7 at the intergenic región between EPA4 and the telomere (pAP471/*Apa*I and *Xba*I)	(De Las Peñas et al., 2003)
CGM147	BG14	*ura3*Δ*::*Tn*903* G418^R Tn7, at the intergenic between *EPA1* and *EPA2, (*pAP508 *SpeI/BcgI)*	(De Las Peñas et al., 2003)
CGM399	BG14	*ura3*Δ::Tn903 G418^R pAP509/*Spe*I integrated between *ISC1* and *HYR1*	(Rosas-Hernández et al. 2008)
CGM397	BG14	*ura3*Δ::Tn903 G418^R pAP430/*Spe*I integrated at the chromosome	(Rosas-Hernández et al. 2008)
CGM4275	BG14	*ura3*Δ::Tn*903* G418^R *URA3*@-791 bp from *EPA1* (Fusion PCR, primers #2823/#2826)	This work
CGM4277	BG14	*ura3*Δ::Tn*903* G418^R *URA3*@-2242 bp from *EPA1* (Fusion PCR, primers #2829/#2832)	This work

CGM4364	BG14	*ura3*Δ::Tn*903* G418^R *URA3*@1 bp from *EPA1* (Fusion PCR, primers #2903/#2820)	This work
CGM4634	CGM118	*ura3*Δ::Tn*903* G418^R *EPA6*::Tn7 986 bp upstream stop codon. pGH14 digested with *Bsg*I/*Mfe*I integrated. (*esc1Δ::*NAT)	This work
CGM4640	CGM121	*ura3*Δ::Tn*903* G418^R *EPA7* 3'UTR::Tn7 268 bp upstream stop codon. pGH14 digested with *Bsg*I/*Mfe*I integrated. (*esc1Δ::*NAT)	This work
CGM4627	CGM159	*ura3*Δ::Tn*903* G418^R Tn7 at the intergenic region between *EPA5* and *EPA4*. pGH14 digested with *Bsg*I/*Mfe*I integrated. (*esc1Δ::*NAT)	This work
CGM4629	CGM160	*ura3*Δ::Tn*903* G418^R Tn7 at the intergenic region between *EPA4* and the telomere. pGH14 digested with *Bsg*I/*Mfe*I integrated. (*esc1Δ::*NAT)	This work
CGM4684	CGM225	*ura3*Δ::Tn*903* G418^R CGM118 pAP612 digested with *Bcg*I and integrated (*hdf1Δ::*hph) pGH14 digested with *Bsg*I/*Mfe*I integrated. (*esc1Δ::*NAT)	This work
CGM4686	CGM227	*ura3*Δ::Tn*903* G418^R CGM118 pAP612 digested with *Bcg*I and integrated (*hdf1Δ::*hph) pGH14 digested with *Bsg*I/*Mfe*I integrated. (*esc1Δ::*NAT)	This work
CGM4704	CGM276	*ura3*Δ::Tn*903* G418^R CGM121 pAP612 digested with *Bcg*I and integrated (*hdf2Δ::*hph) pGH14 digested with *Bsg*I/*Mfe*I integrated. (*esc1Δ::*NAT)	This work
CGM4706	CGM275	*ura3*Δ::Tn*903* G418^R CGM121 pAP612 digested with *Bcg*I and integrated (*hdf1Δ::*hph) pGH14 digested with *Bsg*I/*Mfe*I integrated. (*esc1Δ::*NAT)	This work
Epitope tagged (*MYC/ FLAG*) for ChIP and CoIP			

CGM1236	CGM983	*ura3*Δ::Tn903 G418^R *HST1-MYC* (pOZ32/*XmnI-Blp* I)/*SUM1-FLAG* (pOZ72/*Pvull-Bgl* II) *Hyg^S*	(Orta-Zavalza et al., 2013)
CGM3111	CGM2415	*ura3*Δ::Tn*903* G418^R *RAP1*-Flag	(López-Fuentes et al., 2018)
CGM4377	CGM3588	*abf1Δ::FRT* /pGE238 (pP_{MT1}::*FLAG::ABF1*.URA$^+$)	(Hernández-Hernández et al., 2021)
CGM4091	CGM1107	*ura3*Δ::Tn*903* G418^R pJV22*/BsrGI-HpaI (SIR3::FLAG::FRT)/*pGE242 (pP_{MT1}*::MYC::ABF1)*	This work
CGM4093	CGM1113	*ura3*Δ::Tn*903* G418^R pJV13*/BglII-BcgI (SIR4::FLAG::FRT)/*pGE242 (pP_{MT1}*::MYC::ABF1)*	This work
CGM4095	CGM3111	*ura3*Δ::Tn*903* G418^R *RAP1::FLAG/*pGE242 (pP_{MT1}*::MYC::ABF1)*	This work
CGM4097	CGM1307	*ura3*Δ::Tn*903* G418^R *KU70::FLAG/* pGE242 (pP_{MT1}*::MYC::ABF1)*	This work
CGM4099	CGM1313	*ura3*Δ::Tn*903* G418^R *KU80::FLAG/* pGE242 (pP_{MT1}*::MYC::ABF1)*	This work
CGM4114	CGM3588	*ura3*Δ::Tn*903* G418^R *abf1*Δ*::FRT/* pGH8*(*pP_{MT1}*::MYC::ABF1)/* pGE238 *(* pP_{MT1}*::FLAG::ABF1)*	This work
***GFP* reporter fusions for FACS**			
CGM514	BG14	*ura3*Δ::Tn*903* G418^R pMC14 replicative plasmid	(Gutiérrez-Escobedo et al., 2020)
CGM1936 (BG198)	BG14	*ura3*Δ::Tn*903* G418^R *epa1Δ::GFP* under the control of *EPA1* promoter.	(De Las Peñas et al., 2003)
CGM1937 (BG201)	BG14	*ura3*Δ::Tn*903* G418^R *epa1Δ::GFP* pYlp*lac*211 integrated 300 bp from TAA of *EPA1*. GFP under the control of *EPA1* promoter.	(Gallegos-García et al., 2012)
CGM3705	CGM3703	*ura3*Δ::Tn*903* G418^R *epa1Δ::GFP* under the control of *EPA1* promoter. *silΔ::FRT* pAP430-*Spe*I integrated between *ISC1* and *HYR1*.	(Juárez-Cepeda et al., 2015)

CGM4999	CGM1936	*ura3*Δ::Tn*903* G418^R *epa1Δ::GFP* under the control of *EPA1* promoter. pCI32 digested with *Bsg*I and integrated (*abf1-43*:NAT)	This work
CGM5001	CGM1937	*ura3*Δ::Tn*903* G418^R *epa1Δ::GFP* pYlp*lac*211 integrated 300 bp from TAA of *EPA1*. GFP under the control of *EPA1* promoter. pCI32 digested with *Bsg*I and integrated (*abf1-43*:NAT)	This work
CGM5048	CGM3705	*ura3*Δ::Tn*903* G418^R *epa1Δ::GFP* under the control of *EPA1* promoter. *silΔ::FRT* pAP430-*Spe*I integrated between *ISC1* and *HYR1.* pCI32 digested with *Bsg*I and integrated (*abf1-43*:NAT)	This work
Fluorescent tagged for microscopy (mCherry/GFP/YFP)			
CGM4766	CGM4389	*ura3*Δ::Tn*903* G418^R pGE316 ($P_{MT\text{-}1}$::*GFP*::*PRX1*::T_{HIS3}) Ura$^+$ pGH20 digested with *EcoNI/MfeI* (*NUP49*::*CHERRY*::*NAT*)	This work
CGM4768	CGM1200	*ura3*Δ::Tn*903* G418^R pMS19 digested with *KpnI*/*SpeI* (*HDF1::GFP*) pGH20 digested with *EcoNI/MfeI* (*NUP49*::*CHERRY*::*NAT*)	This work
CGM4770	CGM1109	*ura3*Δ::Tn*903* G418^R pJV22 digested with *BsrGI/HpaI* (*SIR4::GFP)* pGH20 digested with *EcoNI/MfeI* (*NUP49*::*CHERRY*::*NAT*)	This work
CGM4771	CGM1	*ura3*Δ::Tn*903* G418^R pGH20 digested with *EcoNI/MfeI* (*NUP49*::*CHERRY*::*NAT*)	This work
CGM4827	CGM1	*ura3*Δ::Tn*903* G418^R pGH24 ($P_{MT\text{-}1}$::mCherry::*KU80*::T_{HIS3}) *URA+*	This work
CGM4829	CGM1	*ura3*Δ::Tn*903* G418^R pGH24 ($P_{MT\text{-}1}$::*YFP*::*KU80*::T_{HIS3}) *URA+*	This work
CGM4876	CGM1	*ura3*Δ::Tn*903* G418^R pGH27 ($P_{MT\text{-}1}$::mCherry::*NUP49*::T_{HIS3}) *NAT*^{R}	This work
CGM4878	CGM4829	*ura3*Δ::Tn*903* G418^R	This work

		pGH24 ($P_{MT\text{-}1}$::*YFP*::*KU80*::T_{HIS3}) *URA+* / pGH27 ($P_{MT\text{-}1}$::mCherry::*NUP49*::T_{HIS3}) *NAT*^{R}	
CGM4880	CGM1109	*ura3*Δ::Tn*903* G418^R pJV22 digested with *BsrGI/HpaI* (*SIR4::GFP*) / pGH27 ($P_{MT\text{-}1}$::mCherry::*NUP49*::T_{HIS3}) *NAT*^{R}	This work
CGM4882	CGM1200	*ura3*Δ::Tn*903* G418^R pMS19 integrated digested with *KpnI*/*SpeI* (*HDF1::GFP*) pGH27 ($P_{MT\text{-}1}$::mCherry::*NUP49*::T_{HIS3}) *NAT*^{R}	This work

Table S 2 Plasmids

Plasmids	Relevant genotype	Reference
pYC44	Integrative plasmid with cassette de *NAT* (FRT::*NAT*::*3'UTR*$_{CTA}$::FRT) Amp^R	(Yáñez-Carrillo et al., 2015)
pYC54	Integrative plasmid (YFP::NAT) Amp^R	(Yáñez-Carrillo et al., 2015)
pYC56	Integrative plasmid (CHERRY::NAT) Amp^R	(Yáñez-Carrillo et al., 2015)
pMB11	Cloning vector with a single restriction site of *Stu*I, Cm^R/Sac^S	Lab collection
pGH3	PCR fragment of 570 bp cMyc-Linker amplified from pVA59, digested with *Spe*I/*Cla*I cloned into pVA106 digested with *Spe*I/*Cla*I	(Hernández-Hernández et al., 2021)
pGH5	PCR fragment of 1.44 Kb of *ABF1* with *Cla*I sites added, cloned into pMB11 digested with *Stu*I	(Hernández-Hernández et al., 2021)
pGH8	PCR fragment of 1.44 Kb of *ABF1* from pGH5 digested with *Cla*I, cloned into pGH3 digested with *Cla*I	(Hernández-Hernández et al., 2021)
pGH12	PCR fragment of 744 pb amplified with #2774 and #2714 (5'*ESC1*, with site SacI and *BamH*I) clone into pYC44 digested with *Sac*I and *BamH*I.	This work
pGH14	A PCR fragment of 1095 pb amplified with #2716 and #2717 (3'*ESC1*, sites added *Xho*I and *Kpn*I), cloned into pGH12 digested with *Xho*I and *Kpn*I.	This work
pGH17	PCR fragment of 880 pb amplified with #3112 and #3115 (3'ORF-*NUP49* with site *SacII* and *BamHI*) clone into pYC54 digested with *SacII* and *BamHI*	This work
pGH18	PCR fragment of 880 pb amplified with #3112 and #3115 (3'ORF-*NUP49* with site *SacII* and *BamHI*) clone into pYC56 digested with *SacII* and *BamHI*	This work
pGH20	PCR fragment of 604 pb amplified with #3113 and #3114 (3'UTR-*NUP49* with site *XhoI* and *Acc651*) clone into pGH18	This work
pGH22	PCR fragment of 604 pb amplified with #3113 and #3114 (3'UTR-*NUP49* with site *XhoI* and *Acc651*) clone into pGH17	This work
pGH24	PCR fragment of 1.848 Kb amplified with #3195 and #3196 (ORF-KU80 with site *Cla*I and *Sal*I) clone into pVA87 (P$_{MT-1}$::*YFP.URA+*)	This work
pGH25	PCR fragment of 1.848 Kb amplified with #3195 and #3196 (ORF-KU80 with site *Cla*I and *Sal*I) clone into pVA152 (P$_{MT-1}$::mCherry*.URA+)*	This work
pGH27	PCR fragment of 1.515 Kb amplified with #3191 and #3192 (ORF-NUP49 with site *Sal*I and *Xho*I) clone into pVA99 (P$_{MT-1}$::mCherry*.NAT^R)*	This work
pGE80	(pFRT::Sc*URA3*::FRT) CmR ori p15A	(Gutiérrez-Escobedo et al., 2020)
pGE238	PCR fragment of 2.024 Kb released from pVS1digested with *Spe*I/*Kpn*I (P$_{MT1}$::FLAG::ABF1::T$_{HIS3}$), clone into pVA98 digested with *Spe*I/*Kpn*I	(Hernández-Hernández et al., 2021)

Table S 3 Primers

ChIP-qPCR			
Primer (No.)	**Sequence (5'-3')**	**Added sites**	**Hybridation site**
2722	GGTCTTGATGGTGCTTTCTC	None	*EPA2*@-1136 Fw
2723	GTTTAACGTATCGGCCTA	None	*EPA2*@-1264 Rv
2724	ACCCACTAACCGAATTAGGAG	None	*EPA2*@-2411 Fw
2725	CCATCCAGCCAATGCTAATAC	None	*EPA2*@-2606 Rv
2726	GCCAGGTACGCAATTAAAGAC	None	*EPA2*@-3162 Fw
2727	GAACCGCTATGAGTTTACATCACA	None	*EPA2*@-3293 Rv
2728	CCTGTCGAAATAACCAGGTAGG	None	*EPA2*@-3864 Fw
2729	GAAATAGCCACACAGCTGAATGA	None	*EPA2*@-4125 Rv
2736	ACCAAATGCTTCTGGAAAGAAC	None	*EPA1*@-2530 Fw
2737	GAGCACCTTTTAAATGTTAGCCA	None	*EPA1*@-2365 Rv
2738	CGCACTGTCAAGGAATTTGC	None	*EPA1*@-1677 Fw
2739	GGTACCCTGCTAAGTGACACA	None	*EPA1*@-1499 Rv
2740	CATCGAAGAAGGCATTGCAG	None	*EPA1*@-1400 Fw
2741	GTTGTTGATAGCTGCTCAGATT	None	*EPA1*@-1185 Rv
2742	TCCAGTACATGCCAGTTTCG	None	*EPA1*@-941 Fw
2743	GTACGGAATATGCTTTCTAGCG	None	*EPA1*@-692 Rv
2964	ATAGCCATTTCGGCCAGTCC	None	*ABF1*@-364 Fw
2965	TTCGTCGTCAAACTTCTCG	None	*ABF1*@-236 Rv
2972	ATTGCGAAACTATGCATCAC	None	*RAP1*@-640 Fw
2973	GCAGATGGCAGCGTTCTTCAC	None	*RAP1*@-362 Rv
3159	CATACGAAGCCTAATTTGCC	None	*EPA1*@+253 Fw
3160	GCCTTGCACCATAGTCGTAT	None	*EPA1*@+515 Rv
3161	CCGCTCATACAGGCACAGAAG	None	*EPA1*@+524 Fw
3162	GACTATTATCAATGAGGGCTC	None	*EPA1*@+607 Rv
3165	AGAGAGTCTTGTTGCTCGAAC	None	*EPA2*@+984 Fw
3166	CTTGCGAATACACTACCTCT	None	*EPA2*@+825 Rv
3167	AGTGCCCCAACCAAGATTAA	None	*EPA2*@+632 Fw
3168	CAATGTGGCCCTCTATATGA	None	*EPA2*@+485 Rv
2230	GAAACTTCTGAACAGACTACG	None	*EPA3*@-5802 Fw
2231	GACCCCACAGTACCCAGACC	None	*EPA3*@-6034 Rv
2503	GTAGCTGGGTGGTCATCG	None	*ISC1*@1137 Fw
2504	GACTAGCTTGCTGCGGACTC	None	*ISC1*@+71 Rv
Epitope tagged versions			
Primer (No.)	**Sequence (5'-3')**	**Added site**	**Hybridation site**
3110	GCCTCAAGTGGTGGACTCTTTGGC	None	*NUP49*@282 Fw

3111	GAACAGCTACATCACTTGCGATGCC	None	*NUP49*@+828 Rv
3112	CTGTCCGCGGTAAGCCTGCACAAGGAATAGG	SacII	*NUP49*@633 Fw
3113	CGCTCTCGAGACCTCTCAATGTTCAATAGTG	XhoI	*NUP49*@+1 Fw
3114	GATAGGTACCCCTTGCACGCAGCTTGACTTTCAGTTTAG	Acc651	*NUP49*@+583 Rv
3115	CGCGGGATCCCCTTGGTACTAGTCAAAAGTTTCAC	BamHI	*NUP49*@1512 Rv
3191	CTAGCGTCGACATGTTTGGGGCTAAATAAACCTTCTACAG	SalI	*NUP49*@1 Fw
3192	TCGATCTCAGCTACTTGGTACTAGTCAAAAG	XhoI	*NUP49*@1515 Rv
3195	CTAGATCGATATGTCGGAAGCCACAT	ClaI	*KU80*@1 Fw
3196	TAGCGTCGACTTATGACTCCCCTTCTCTTGC	SalI	*KU80*@1848 Rv
3197	GGACTACTTCGGCAAGCGCA	None	*KU80*@318 Fw
3198	TCCACTATGTTCTCCAGGCTG	None	*KU80*@644 Rv
***URA3* fusions**			
Primer (No.)	**Sequence (5'-3')**	**Added site**	**Hybridation site**
2822	ACTCAACAATTCACTCTACTACC	None	*EPA1*@-2506 Fw
2823	GAATTGTACCTGGCTAATGC	None	*EPA1*@-2446 Fw
2824	CGAATTCAGGAACTTGATATTTTTAATTAGGATTATTACCGTTAACAG	None	*EPA1*@-1782 Rv
2825	GGCTACCACATCGTCTTTGAACATTAGTGAAAATCAGTACAT	None	*EPA1*@-791 Fw
2826	CCATATTATGATCGCATGCT	None	*EPA1*@-343 Rv
2827	GTAGGATAGAGTAAATAAATCTGC	None	*EPA1*@-220 Rv
2831	GGCTACCACATCGTCTTTGATTATGTCAAGCTTGAACATTAA	None	*EPA1*@-2242 Fw
2832	TGTTGATAGCTGCTCAGATTCAG	None	*EPA1*@-1209 Rv
2833	CGTTCACCGAGTATTCAGTACAT	None	*EPA1*@-1120 Rv
2828	ATAGCAGCCGTTACTTGAATG	None	*HYR1*@2336 Fw
2829	ACAACTCTTGATAATAAGTC	None	*HYR1*@2617 Fw
2830	CGAATTCAGGAACTTGATATTTTTTTGTGACAGCAAAAAGGAAAAG	None	*HYR1*@+464 Rv
604	AAAAATATCAAGTTCCTGATTTCG	None	Sc*URA3* cassette
605	CAAAGACGATGTGGTAGCC	None	Sc*URA3* cassette
RT-qPCR			
Primer (No.)	**Sequence**	**Added site**	**Hybridation site**
219	CGCCGGTGACGATGCTCC	None	*ACT1*@70Fw
977	CGTTGTAGAAAGTGTGATGC	None	ACT1@258Rv
22	TAACAGTGTTTTCGTTTGAT	None	*EPA1*@717 R*v*
36	GGGCTCAAAAACAGCTAAAG	None	*EPA1*@594 Fw
1268	GAATCTTGGTGCTGGAAATGC	None	*EPA2*@480Fw
1269	TGGACATTGCTCTTCATCAGA	None	*EPA2*@739Rv
38	GCATGTTGATAGTTCCAAAA	None	*EPA3*@573 Rv
24	TAATTTGATCAGTAGCACCG	None	*EPA3*@715 Fw
***NAT* cassette**			
569	TACAAAGCTTGTTCACCATCGGAAGC	None	Nourseotricine cassette Rv
1096	GCTTGCCTCGTCCCCG	None	Nourseotricine cassette Fw